

METAL COMPLEXATION OF BILIRUBIN AND ITS  
DIMETHYL ESTER IN N,N-DIMETHYLFORMAMIDE

by

Edward T. Yatsko

Submitted in Partial Fulfillment of the Requirements  
for the Degree of  
Master of Science  
in the  
Chemistry  
Program

John D. Van Patten March 8, 1977  
Advisor Date

John Raul March 9, 1977  
Dean of the Graduate School Date

YOUNGSTOWN STATE UNIVERSITY

March 1977

## ABSTRACT

METAL COMPLEXATION OF BILIRUBIN AND ITS  
DIMETHYL ESTER IN N,N-DIMETHYLFORMAMIDE

Edward T. Yatsko

Master of Science

Youngstown State University, 1977

This study deals with the formation and identification of bilirubin-metal complexes in the solvent N,N-Dimethylformamide, DMF. Extensive qualitative experiments were performed in order to discover metal salts that would react with bilirubin to give a shift in the well known visible spectrum of bilirubin. A fair number of such metal salts were found but only after a great deal of trial and error. There were a number of reasons for the difficulty in finding these bilirubin-metal complexes. Among these were: 1) the rapid decomposition of DMF, 2) the change in the oxidation state of some metal ions in DMF, 3) the nature of the anion of the metal salt, 4) the acid-base equilibria of bilirubin in DMF, 5) the crucial molar ratios of bilirubin:base:metal to form complexes, 6) the sensitivity of both bilirubin and DMF to light, and 7) the solubility of metal salts in DMF, all of which will be discussed in some detail.

From this qualitative work it was found that two different types of spectral shifts in the bilirubin

(450 nm) visible spectrum occurred. One termed the "Zn type" is the shift of the bilirubin maximum absorbance peak to longer wavelengths and the other termed the "Al type" is the shift of the bilirubin (450 nm) maximum to shorter wavelengths. Based on this spectral phenomenon of two different shifting patterns of bilirubin's absorbance peak and supported by work with bilirubin dimethyl ester, ethylenediamine, 2,4-pentadione and the quantitative formation of metal complexes, it is proposed here that there are at least two distinct structures for bilirubin-metal complexes in DMF. The techniques used to prepare materials and to analyze the complexes formed will also be discussed. These include visible spectroscopy, potentiometric titrations, polarography, esterification of bilirubin, purification and standardization of the DMF solvent system and fluorometry.

## ACKNOWLEDGEMENTS

I would like to thank Dr. John D. Van Norman, my thesis advisor, for his excellent suggestions, guidance and support throughout this project. I would next like to thank Dr. Inally Mahadeviah, Dr. Thomas Dobbelstein, Dr. Leonard Spiegel and Dr. Richard Phillips for their helpful discussions of this material. My gratitude also goes to Dr. Elmer Foldvary for stirring my enthusiasm toward chemistry by his fine manner of teaching and Dr. James Reeder for helping me to improve my lab techniques in his organic synthesis laboratory.

I.	THE PROBLEM	2
II.	THEORY	4
	A. Novel Ion-Pairs Complexation	4
	B. Visible Spectroscopy	10
	C. Potentiometric Titrations	11
	D. Polarography	12
	E. Fluorometry	15
III.	MATERIALS AND APPARATUS	17
	A. Materials and Apparatus	17
IV.	EXPERIMENTAL PROCEDURE AND RESULTS	22
	A. Purification of BHP	22
	B. Standardization of the BHP System	24
	C. Esterification of Bilirubin	32
	D. Qualitative Complexation of Bilirubin and Bilirubin Dimethyl Ester with Metal Salts	33

## TABLE OF CONTENTS

	PAGE
ABSTRACT . . . . .	ii
ACKNOWLEDGEMENT . . . . .	iv
TABLE OF CONTENTS . . . . .	v
LIST OF SYMBOLS . . . . .	vii
LIST OF FIGURES . . . . .	ix
CHAPTER	
I. INTRODUCTION . . . . .	1
A. Background . . . . .	1
B. Statement of the Problem . . . . .	2
II. THEORY . . . . .	4
A. Metal Ion-Ligand Complexation . . . . .	4
B. Visible Spectroscopy . . . . .	10
C. Potentiometric Titrations . . . . .	11
D. Polarography . . . . .	12
E. Fluorometry . . . . .	15
III . MATERIALS AND APPARATUS . . . . .	18
A. Materials and Apparatus . . . . .	18
IV. EXPERIMENTAL PROCEDURE AND RESULTS . . . . .	22
A. Purification of DMF . . . . .	22
B. Standardization of the DMF System . . . . .	24
C. Esterification of Bilirubin . . . . .	32
D. Qualitative Complexation of Bilirubin and Bilirubin Dimethyl Ester with Metals Salts . . . . .	33

## TABLE OF CONTENTS (CON'T)

CHAPTER	PAGE
E. Quantitative Complexation of Bilirubin and Bilirubin Dimethyl Ester with Zinc and Aluminum Salts . . .	49
F. Polarography of Copper Salts in DMF .	54
G. Fluorometry of Bilirubin and Bilirubin Dimethyl Ester and Their Complexes . . . . .	57
V. DISCUSSION AND CONCLUSIONS . . . . .	58
REFERENCES . . . . .	62

$C$	Concentration	mole/liter
$T$	Temperature	degrees centigrade
$D$	Diffusion coefficient	centimeters <sup>2</sup> /second
DMF	N,N-Dimethylformamide	
DME	Dropping mercury electrode	
$E_{1/2}$	Half-wave potential	volts
$\epsilon$	Molar absorptivity	liter/mole-centimeter
$E_{cell}$	Cell potential	volts
$E_g$	Potential measured at a glass membrane electrode	volts
$E_{ref}$	Standard electrode potential	volts
$E_{ref}$	Electrode potential of any arbitrary reference electrode	volts
$F$	Faraday constant	96,487 coulombs/equivalent

## LIST OF SYMBOLS

SYMBOL	DEFINITION	UNITS
A	Absorbance	
a	Absorptivity	grams/liter
b	Internal path length in cell	centimeters
BR	Bilirubin	
BRDME	Bilirubin Dimethyl Ester	
BV	Biliverdin	
C	Concentration	millimoles/ liter
c	Concentration	moles/liter
$^{\circ}\text{C}$	Temperature	degrees centi- grade
D	Diffusion coefficient	centimeters <sup>2</sup> / second
DMF	N,N-Dimethylformamide	
DME	Dropping mercury electrode	
$E_{1/2}$	Half-wave potential	volts
e	Molar absorptivity	liter/mole- centimeter
$E_{\text{cell}}$	Cell potential	volts
$E_{\text{g}}$	Potential measured at a glass membrane electrode	volts
EN	Ethylenediamine	
$E^{\circ}_{\text{ox,red}}$	Standard electrode potential	volts
$E_{\text{ref}}$	Electrode potential of any arbi- trary reference electrode	volts
F	Faraday constant	96,487 cou- lombs/equiva- lent

## LIST OF SYMBOLS (CONT'D)

SYMBOL	DEFINITION	UNITS
Fl	Power of fluorescence	
K	Instrument, system constant	
K'	2.30 K	
M	Molar	moles/liter
m	Rate flow of mercury	milligrams/ second
mmols	Millimoles	millimoles
ml	Millimeters	millimeters
mv	Millivolts	millivolts
n	Number of moles of electrons exchanged per mole of reactant	equivalent/ mole
nm	Nanometers	nanometers
PA	Picric acid	
P	Power of transmitted radiation	
2,4-PDO	2,4-Pentadione	
P <sub>o</sub>	Power of incident radiation	
R	Universal gas constant	
T	Temperature	Kelvin units
<u>T</u>	Transmittance	
t	Any time during a drop life	seconds
TB	Tetrabutylammonium hydroxide	
TMG	Tetramethylguanidine	
ua	Microamps	microamperes
UV	Ultra violet radiation	
V,v	Volts	volts



## LIST OF FIGURES

FIGURE	PAGE
1. A: Bis-lactam Structure of BR with eight possible donor sites numbered B: Bis-lactim Structure of Neutral BR . . . . .	5
2. Potentiometric Titration of PA with TB . . .	25
3. First Derivative Plot for the Titration of PA with TB . . . . .	26
4. Potentiometric Titrations of PA and $AlCl_3$ with TMG . . . . .	27
5. Potentiometric Titration of BR with TB . . .	28
6. Potentiometric Titration of $AlCl_3$ with TB .	30
7. Potentiometric Titrations of DMF with TMG and TB . . . . .	31
8. Visible Spectra of BR/TB/ $CuCl$ /DMF . . . . .	35
9. Visible Spectra of Acid-Base Behavior of BR in DMF . . . . .	35
10. Visible Spectra of Acid-Base Behavior of BRDME in DMF and in $HCCl_3$ . . . . .	36
11. Visible Spectra of BR/TMG/ $ZnI_2$ /DMF . . . . .	36
12. Visible Spectra of BR/TMG/ $CdAc_2 \cdot 2H_2O$ /DMF . . .	39
13. Visible Spectra of BR/TMG/ $AlCl_3$ /DMF . . . . .	39
14. Visible Spectra of BR/TMG/ $MgCl_2 \cdot 6H_2O$ /DMF . . .	40
15. Visible Spectra of BR/TB/ $PbCl_2$ /DMF . . . . .	40
16. Visible Spectra of BR/TB/ $SnCl_2 \cdot 2H_2O$ /DMF . . .	41
17. Visible Spectra of BR/TB/ $AgNO_3$ /DMF and BR/TMG/ $AgAc$ /DMF . . . . .	41
18. Visible Spectra of BRDME/TMG/ $ZnI_2$ /DMF . . .	42
19. Visible Spectra of BRDME/TMG/ $CdAc_2 \cdot 2H_2O$ /DMF . . . . .	42

## LIST OF FIGURE (CONT'D)

FIGURE	PAGE
20. Visible Spectra of BRDME/TMG/ $\text{AlCl}_3$ /DMF . . . . .	43
21. Visible Spectra of BRDME/TMG/ $\text{MgCl}_2 \cdot 6\text{H}_2\text{O}$ / DMF . . . . .	43
22. Likely Structure for $\text{Zn}_2$ -BR . . . . .	46
23. Likely Structure for $\text{Zn}_3$ -BR . . . . .	46
24. Likely Structure for $\text{Al}_3$ -BR <sub>2</sub> . . . . .	47
25. Neutral BR drawn in two planes with intra- molecular hydrogens bonds supporting the planarity of the molecule . . . . .	47
26. Spectrophotometric Titration of BR/TMG with $\text{ZnI}_2$ /DMF . . . . .	50
27. Spectrophotometric Titration of BRDME/TMG with $\text{ZnI}_2$ /DMF . . . . .	52
28. Spectrophotometric Titration of BR/TMG with $\text{AlCl}_3$ /DMF . . . . .	52
29. Spectrophotometric Titration of BRDME/TMG with $\text{AlCl}_3$ /DMF . . . . .	53
30. Polarogram of $\text{CuCl}$ in DMF . . . . .	55
31. Polarogram of $\text{CuCl}_2$ in DMF . . . . .	56

## CHAPTER I

## INTRODUCTION

A. Background

Medical researchers have shown great interest in the yellow linear tetrapyrrole bile pigment called bilirubin, hereafter referred to as BR. This is because BR is an important product of hemoglobin degradation in the liver, spleen and bone marrow as elucidated by Szentirmay.<sup>1</sup> If BR is not further broken down by the liver, disease conditions such as jaundice result. Van Norman and Szentirmay<sup>2,3,4</sup> demonstrated that DMF was a good solvent for electroanalytical and spectrophotometric studies of BR. Szentirmay<sup>5</sup> quantitatively formed BR/TMG/Zn<sup>++</sup>/DMF complexes. Szentirmay's work with Zn-BR complexes comprised most of the background for this study.

As Szentirmay<sup>6</sup> reported, very little recent analytical work on BR was found in the literature even though there was found a tremendous number of other kinds of BR studies. Some studies that did overlap this study are: Mark's<sup>7</sup> work with the fluorescence of bilirubin dimethyl ester, hereafter referred to as BRDME; Jirsa's et al.<sup>8</sup> work with BRDME and glucuronic acid; Kolthoff's et al.<sup>9</sup> discussion on metal-ligand complexation; Kolthoff's et al.<sup>10</sup> work with acid-base strength in DMF; Lee's et al.<sup>11</sup>

work with BR ionic equilibria; Velapoldi and Menis's<sup>12</sup> work with BR-metal complexes; Hutchinson's et al.<sup>13</sup> work with BR-metal complexes; Kuenzle's et al.<sup>14</sup> work with BR-metal complexes; Cu's et al.<sup>15</sup> work on the fluorescence of BR; Hutchinson's et al.<sup>16</sup> preparation of BRDME; Cotton and Wilkinson's<sup>17</sup> discussion of metal-ligand complexation; Durrant and Durrant's<sup>18</sup> discussion of metal-ligand complexation; Bailar's<sup>19</sup> discussion of metal-ligand complexation; Mercer and Truter's<sup>20</sup> work with the complexation of specific large ligands and alkali metals; Pauling's<sup>21</sup> discussion of hybridization upon complexation; Manitto and Monti's<sup>22</sup> work on the hydrogen bonding in the BR molecule; Kuenzle's et al.<sup>23</sup> work on the hydrogen bonding in the BR molecule.

### B. Statement of the Problem

This study is an investigation into BR-metal complexes in DMF using primarily visible spectroscopy and also using potentiometric titrations, polarography and fluorometry. The initial problem was to find some BR-metal complexes in DMF and then to identify them. However, once a number of such complexes were found using visible spectroscopy, it became quite interesting to attempt to determine their structures. This new problem was also approached primarily using visible spectroscopy. BRDME was prepared and used as a tool in order to determine the sites of attachment of the metals to BR. Decomplexation

back to BR was also important because it showed that it was indeed the interaction of the metal with BR which shifted the BR spectrum.

Several preliminary problems had to be solved before any meaningful investigation into the formation of BR-metal complexes could be made. These included the standardization of the DMF solvent system and the acid-base equilibria of BR in DMF. The determination of a good technique for the purification and storage of DMF was the beginning step. Potentiometric titrations were then performed to standardize the bases, TMG and TB, and to investigate BR's protons which needed to be removed to obtain any BR-metal complexation.

This study of BR-metal complexes was undertaken because of the great importance of BR in biological systems. Also many other molecules in living systems have structures similar to that of BR. Metal complexation of BR could aid scientists to better understand the structures and functions of BR and other similar molecules. From such additional knowledge about the chemistry of BR, new methods of analyzing and controlling levels of BR and similar molecules found in living systems could possibly be found.

## CHAPTER II

## THEORY

A. Metal Ion-Ligand Complexation

Metal ion complexation chemistry basically involves the reaction of a central metal cation with a number of anionic or neutral ligands that possess at least one free lone pair of electrons that can be used in bonding. This section discusses some theories which pertain to metal ion complexation chemistry involving primarily polydentate ligands similar to BR and BRDME. Figure 1 shows the structure of BR, the lactam-lactim tautomerism of BR and the eight possible sites on BR which could be complexed by a metal cation. These eight sites or donor atoms which could complex a metal ion are the two COO-groups, the four pyrrole nitrogens and the two lactam-lactim oxygens on the two outside pyrrole rings. However there are only six protons in the neutral BR molecule that can possibly be removed in complexation.<sup>3</sup> Four protons are felt to be removable by the addition of base.<sup>11</sup> The other two protons which can not be removed by the addition of base may be stabilized by the tautomerism reported on the lactam-lactim oxygens.<sup>12</sup>

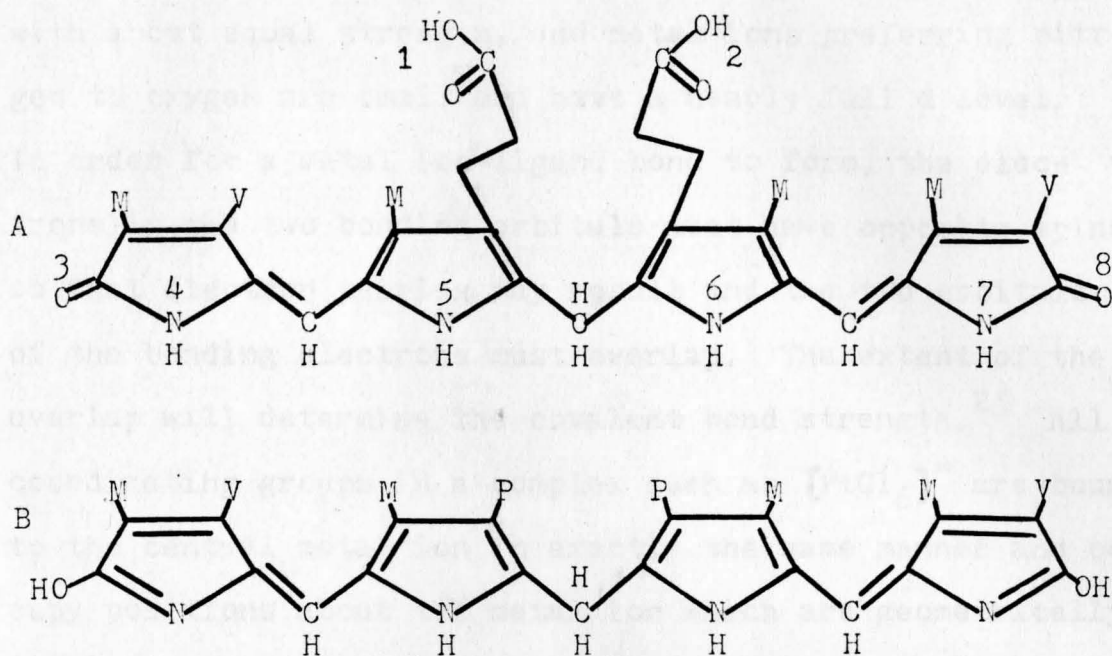


Figure 1. A: Bis-lactam Structure of BR with eight possible donor sites numbered B: Bis-lactim Structure of Neutral BR.

Some important factors affecting the stability of metal ion-ligand complexes are the bond strengths, the chelate effect, the template effect, steric effects and the pH of the solution. The most important factor is the strength of the bonds between the metal ion and the donor atoms. These bonds are generally coordinate covalent bonds in which ligand atoms donate a pair of electrons into the metal ions empty orbitals. Bailar<sup>24</sup> states that metals usually combine with oxygen through normal covalent bonds and with nitrogen through a coordinate covalent bond. He goes on to say that the metal ions that prefer oxygen to nitrogen are nearly all of the inert gas type, beryllium and the larger transition ions bond to oxygen and nitrogen

with about equal strength, and metal ions preferring nitrogen to oxygen are small and have a nearly full d level. In order for a metal ion-ligand bond to form, the electrons in the two bonding orbitals must have opposite spins so that electron pairing may result and the two orbitals of the bonding electrons must overlap. The extent of the overlap will determine the covalent bond strength.<sup>25</sup> All coordinating groups in a complex such as  $[\text{PtCl}_6]^-$  are bound to the central metal ion in exactly the same manner and occupy positions about the metal ion which are geometrically equivalent. Thus the atomic orbitals involved must differ from each other only in direction. Since there are usually an insufficient number of equivalent bonding orbitals available hybridization theory came about. Outer electronic levels which differ little in energy can be changed or broken down and new equivalent bonding or hybridized orbitals can be formed.<sup>26</sup>

$\text{Zn}^{++}$  having a completely filled 3d sublevel generally utilizes 4s and 4p sublevel orbitals in forming complexes. Hence  $\text{Zn}^{++}$  forms  $sp^3$  hybrid orbitals in most of its complexes.<sup>27</sup> Pauling correlated  $sp^3$  hybridization with tetrahedral structure.<sup>28</sup> Stoichiometrically there is only one oxide of aluminum,  $\text{Al}_2\text{O}_3$ .<sup>29</sup> Since the 2s and 2p sublevels of  $\text{Al}^{+++}$  are filled,  $\text{Al}^{+++}$  must utilize hybrid 3s and 3p sublevel orbitals to form this alumina structure. However both tetrahedral and octahedral  $\text{Al}^{+++}$  complexes are



known. Electron deficient complexes in which  $\text{Al}^{+++}$  is tetrahedrally hybridized also utilize 3s and 3p sublevel orbitals<sup>30</sup> as in the Pauling<sup>31</sup>  $sp^3$  hybridization. No chelate compounds have been reported in which  $\text{Al}^{+++}$  is in the tetrahedral bonding state.<sup>32</sup> Chelate compounds have been reported in which  $\text{Al}^{+++}$  is octahedrally hybridized utilizing empty 3d level orbitals<sup>33</sup> as in the Pauling<sup>34</sup>  $d^2sp^3$  hybridization.

Kolthoff et al.<sup>35</sup> also delineated some trends of metal ion-ligand complexation based on electronic structures. The more noble and the less electronegative the donor atom of the ligand, the more stable the complex. They stated that  $\text{Al}^{+++}$  and  $\text{Mg}^{++}$  are strongly oxyphilic and combine with chromogenic organic reagents containing -OH groups.  $\text{Zn}^{++}$ ,  $\text{Cd}^{++}$ ,  $\text{Ag}^+$ ,  $\text{Sn}^{++}$  and  $\text{Pb}^{++}$  are mildly oxyphilic and  $\text{Zn}^{++}$ ,  $\text{Cd}^{++}$  and  $\text{Ag}^+$  form strong ammine complexes while  $\text{Al}^{+++}$ ,  $\text{Mg}^{++}$ ,  $\text{Sn}^{++}$  and  $\text{Pb}^{++}$  show little tendency to combine with amines.

When a metal ion attaches at one site of a polydentate ligand a template effect often comes into play. The first complexing site on the large ligand holds the metal ion in close contact with the ligand so that the rest of the sites can more easily form their bonds to the metal ion. Thus ligand sites that are normally not too reactive to a particular metal ion do bond with that metal ion. When a ring is formed enhancing the stability of the complexation between a metal ion and a polydentate ligand,

it is referred to as a chelate effect. Chelation is dependant on the size of the ring formed and the coordination number of the metal ion. If distortions occur when a metal ion fulfills its coordination number the stability of the resulting complex is lowered. The chelate effect is most pronounced when five- and six-membered rings can be formed.<sup>36</sup> Steric effects become a factor if ligands are too large to fulfill the coordination number of a metal ion or if a metal ion is too large or too small to form a given complex. Mercer and Truter's<sup>20</sup> cage ligands for particular alkali metals demonstrate a steric effect. They showed by determining crystal structures that only specific size metals can complex particular cage ligands.

There is the well known pH effect in which particular metal ion-ligand complexations occur best within certain pH ranges. Complexation formation constants are often calculated for many simple monodentate ligands as well as for certain polydentate ligands, such as EDTA, to various metal ions. This study is primarily concerned with polydentate ligands since BR is this type of ligand. The Zn-EDTA complex has a maximum formation constant value when the pH is approximately 9 and the Al-EDTA complex has its maximum formation constant value when the pH is approximately 5.<sup>37</sup> EDTA contains both oxygen and nitrogen donors. Analytical separations are often performed based on particular different optimum pH values for different metal ions.

Finally, the yellow color of BR has been attributed

to the delocalized electrons in BR's four pyrrole rings.<sup>4</sup> Any influence which would increase the amount of electron delocalization in a molecule should increase the stability of that molecule. Increased stability means lower molecular energy which in turn corresponds to radiation of longer wavelengths.<sup>38</sup> Van Norman<sup>4</sup> has discussed the spectral shifts due to the changes in the number of conjugated double bonds for the molecules of the Gmelin oxidation sequence. In the yellow BR molecule there are five conjugated double bonds in the two pyrrole rings on each side of the methylene bridge. This arrangement absorbs visible light near wavelengths of 450 nm. The green BV molecule which has ten conjugated double bonds absorbs light near 640 nm. Purpurin which has eight conjugated double bonds absorbs light around 570 nm and the yellow molecule, choletelin, again absorbs light near 450 nm like BR. Hence, the more electron dispersion present in the BR system, the longer is the wavelength of the absorbance peak.

## B. Visible Spectrophotometry

The principal instrument used in this study was the Beckman Double Beam Spectrophotometer, the Beckman DB. The light sources of the Beckman DB are a six volt tungsten lamp and a hydrogen lamp for ultra violet, UV, work. This dual light system provides a light source that is effective over a range of wavelengths from around 200 to 800 nm. Therefore by the combination of variable slit widths and focussing mirrors the Beckman DB is capable of high resolution spectral scanning.

The output of the Beckman DB read on a meter on the instrument and/or a recorder attached to the instrument is on an absorbance or transmittance scale. By Beer's law,  $A = abc$  or  $-abc$  or  $-\log T$  or  $2 - \log \%T$  or  $-\log P/P_0$ , one can calculate the concentration of a sample. Beer's law mathematically is easy to apply when only one species is present in the sample being tested. Its only true error occurs when the index of refraction changes due to a change in concentration which is rare under normal working conditions, less than  $10^{-2}$  M. However there are a number of factors that can produce apparent deviations from Beer's law. These include: 1) impurities in the sample, 2) non-monochromatic light, 3) non-linear amplification, 4) reading and instrumental errors, 5) equilibrium effects such as dimerization, pH, complexation, ion interaction, temperature, etc., and 6) solvent effects. By working at low

concentrations the chemical effects can be minimized. By using the Beckman DB, many BR reactions can be followed and instrumental error is greatly reduced from that of a single-beam instrument.

### C. Potentiometric Titrations

Potentiometric titrations are often used to follow the change of potential between the electrodes of a galvanic cell as a function of the amount of titrant added. Kolthoff et al.<sup>10</sup> attested that a glass electrode is effective for potentiometric titrations in DMF. Normal titrations initially show very gradual changes in potential. Then at an equivalence or end point, normal titrations show rapid changes in potential for only small additions of titrant. Potentiometric titrations were used in this study to follow the removal of protons by the two bases, TB and TMG. Bases are generally standardized by weighing out a given amount of an acid and titrating this acid with the bases of unknown concentrations.

The Nernst equation,

$$E_{\text{cell}} = E^{\circ}_{\text{ox,red}} + \frac{RT}{nF} \ln \frac{[\text{Ox}]}{[\text{Red}]} - E_{\text{ref}},$$

is very useful in following potentiometric titrations. At an equivalence point, by the Nernst equation, a quantitative relationship can be obtained between the rapid change in potential and the concentration of an ion in solution. For this study a glass, pH-sensitive electrode was used as the indicator electrode. It measures a potential which is proportional to the difference of the proton concentrations on its inside and outside surfaces. A Ag/AgCl electrode was used as the reference electrode and  $\text{NaClO}_4$  was used as a supporting electrolyte. For this system, the following form of the Nernst equation is applicable:

$$E_g = \frac{RT}{F} \ln \frac{[\text{H}^+]_{\text{unknown}}}{[\text{H}^+]_{\text{standard}}}$$

or

$$E_g = .059 \log \frac{[\text{H}^+]_{\text{unknown at } 25^{\circ} \text{ C.}}}{[\text{H}^+]_{\text{standard}}}$$

First and second derivative plots can be made to accurately locate equivalence points.

#### D. Polarography

Polarography is voltammetry at a dropping mercury electrode (DME). Generally the potential is varied and a current response which is proportional to a chemical reaction occurring at the working electrode is recorded. A plot of current vs potential is the output on the recorder.

From this graph the current can be read and used to calculate the concentration of the original electroactive species by certain equations. Very often the Ilkovic equation,<sup>39</sup>

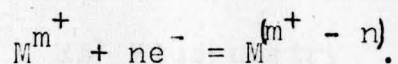
$$i_d = 607 n m^{2/3} t_m^{1/6} D^{1/2} C$$

or

$$(i_d)_M = 708 n m^{2/3} t_m^{1/6} D^{1/2} C$$

where  $i_d$  is the average diffusion or faradaic current,  $(i_d)_M$  is the maximum diffusion current,  $n$  is the number of electrons transferred,  $m$  is the rate of flow of the mercury,  $t$  is the drop time,  $D$  is the diffusion coefficient and  $C$  is the concentration of the electroactive species, is used to find the concentration of an electroactive species in solution. However, very often a polarogram is also used to find an  $E_{1/2}$  value which is characteristic of the half reaction occurring at the working electrode. Polarography is used in this study to find such  $E_{1/2}$  values characteristic of metal ions going from one oxidation state to another. More specifically,  $E_{1/2}$  values were used to see what oxidation state particular metal ions were in when they were dissolved in DMF before being reacted with BR.

The set up used in this study consisted basically of a DME for the working electrode and a Ag/AgCl reference electrode. The current was recorded as a function of applied potential using a Sargent Model XII Polarograph. The generalized reaction that takes place at the working electrode is the cathodic reaction which follows:



Many reduction reactions of this form have characteristic  $E_{1/2}$  values for specific metal ions in a given solvent.

Some of the advantages of polarography include: 1) a constantly renewed reaction surface which provides a relatively constant and thin diffusion layer so that the electrode surface is not effected by past reactions and so that convection and migration are minimized, 2) a high hydrogen overvoltage so that the hydrogen wave is shifted to more negative potentials beyond most  $M^{m+}$  waves, 3) mercury forms amalgams with many metals thereby increasing their solubilities, 4) a good working range for many metal ions where  $i_d$  or  $E_{1/2}$  readings can be taken with relatively good accuracy, sensitivity and resolution, 5) a polarogram can be obtained quickly once a polarograph is set up. Some of the drawbacks of polarography include: 1) a charging current due to drop expansion which interferes with readings of faradaic current, 2) mercury is both toxic and expensive, 3) polarographs are bulky and time consuming to set up, 4) mercury decomposes at +.4 V limiting anodic work, 5) a line through the jagged polarogram must be drawn in order to interpret  $i_d$  or  $E_{1/2}$  readings, and 6) often a surfactant is needed to reduce surface effects.



### E. Fluorometry

Fluorescence is the property of certain materials in which UV radiation is absorbed at a specific wavelength and emitted at a second wavelength. For the Turner Model 430 Spectrofluorometer used here, a xenon lamp provides the source of UV radiation. The xenon lamp puts out a strong continuous spectrum with minor, quite broad lines over the range of 250 nm to 700 nm. The photomultiplier is sensitive to wavelengths from 300 nm to 700 nm for emitted light. The monochromators are highly efficient over the wavelength range from below 200 nm to above 1000 nm. A band width of 15 nm was set with these monochromators so that scattered light due to turbidity in the sample or scattered by the cuvette walls would be removed by the secondary monochromator. Quartz cuvettes with a transmittance range of 250 nm to 1000 nm were used so that UV light could pass. The reference blank of DMF showed very little if any fluorescence and what was seen was blanked out.

In the range of 100 nm to 800 nm the absorption of a photon of light raises one electron of the sample molecule to a higher energy state. The return to ground state is accompanied by the emission of a photon. In solution there is generally a loss of vibrational and/or rotational energy before the return to ground state so that the emitted photon has less energy which corresponds to a peak

at a longer wavelength than the absorbance peak. Unlike phosphorescence, in which there is a notable time delay before emission, fluorescence usually has a very short time interval between absorption and emission.

Fluorometry is often very useful for the analysis of very dilute solutions which show fluorescence. At low concentrations,  $10^{-2}$  M and lower, the absorbed light may be considered proportional to the concentration by the equation,

$$Fl = P_0 K (1 - 10^{-A}),$$

for a single absorbing and fluorescing species, and by the equation,

$$Fl = P_0 K ( 2.30A - (2.30A)^2/2! + (2.30A)^3/3! - \text{etc.} ),$$

for more than one species. At low concentrations the squared term becomes negligible and

$$Fl = 2.30 P_0 K A = P_0 K' a b c,$$

where  $Fl$  is the power of the fluorescence reaching the detector,  $P_0$  is the power of the incident UV radiation,  $K$  is a constant for a given system and instrument,  $A$  is the absorbance of the solution at the primary wavelength,  $K'$  is  $2.30 K$ ,  $a$  is absorptivity and  $b$  is the path length in the primary direction. In this study however fluorometry was used to determine fluorescent patterns characteristic of BR alone and with various metal ions or groups attached to it. The excitation wavelength was set and a scan for an

emission peak was performed. Then the fluorometer was set at the maximum emission wavelength and a scan for a more precise excitation wavelength was taken. Finally when the best excitation wavelength possible was decided upon, this excitation wavelength was set on the spectrofluorometer and a final scan for an optimum emission wavelength was run.

Most of the chemicals used in this study were of reagent grade. The DMF however, was dried as 99% pure and has a molar absorptivity of  $51,100 \pm 600$  l. DMF. The DMF was prepared by the method outlined in chapter IV. Also in chapter IV is a description of the purification of the primary solvent used, DMF. Table I lists the chemicals used in this study.

Following are the apparatus used: 1) a Mettler semi-micro balance readable to  $10^{-5}$  g for quantitative measurements, 2) a Beckman DU spectrophotometer for analytical work, 3) a digital pH meter with a pH-sensitive glass electrode for potentiometric titrations, 4) a Jargent Model 41 Polarograph, 5) a Turner Model 430 Spectrofluorometer for fluorometry, 6) a standard still under a vacuum and an argon atmosphere for DMF purification, and 7) a stirred reaction flask under argon, a laboratory funnel, a filtration flask under a vacuum, an alumina column, and a rotary evaporator for DMF synthesis. Appropriate glassware, pipets, electrodes, hoses, etc. were used where needed.

## CHAPTER III

## MATERIALS AND APPARATUS

A. Materials and Apparatus

Most of the chemicals used in this study were of reagent grade. The BR however was listed as 99% pure and had a molar absorptivity of  $61,100 \pm 600$  in DMF. The BRDME was prepared by the method outlined in chapter IV. Also in chapter IV is a description of the purification of the primary solvent used, DMF. Table I lists the chemicals used in this study.

Following are the apparatuses used: 1) a Mettler semi-micro balance readable to  $10^{-5}$  g for quantitative measurements, 2) a Beckman DB Spectrophotometer for spectral work, 3) a digital pH meter with a pH-sensitive glass electrode for potentiometric titrations, 4) a Sargent Model XII Polarograph, 5) a Turner Model 430 Spectrofluorometer for fluorometry, 6) a standard still under a vacuum and an argon atmosphere for DMF purification, and 7) a stirred reaction flask under argon, a separatory funnel, a filtration flask under a vacuum, an alumina column, and a rotary evaporator for BRDME synthesis. Appropriate glassware, pipets, electrodes, hoses, etc. were used where needed.

TABLE I  
CHEMICALS USED

Material	Formula	Manufacturer
Zinc iodide	$ZnI_2$	Fisher Scientific
Lead chloride	$PbCl_2$	"
Cobalt acetate ( $CoAc_2$ )	$Co(CH_3COO)_2 \cdot 4H_2O$	"
Cupric sulfate (anhydrous)	$CuSO_4$	"
Cadmium chloride	$CdCl_2 \cdot 2.5H_2O$	"
Ferrous sulfate	$FeSO_4 \cdot 7H_2O$	"
Aluminum chloride (anhydrous)	$AlCl_3$	"
Cobalt chloride	$CoCl_2 \cdot 6H_2O$	"
Nickel acetate ( $NiAc_2$ )	$Ni(CH_3COO)_2 \cdot 4H_2O$	"
Nickel chloride	$NiCl_2 \cdot 6H_2O$	"
Nickel carbonate	$NiCO_3$	"
Sodium bicarbonate	$NaHCO_3$	"
Sodium sulfate (anhydrous)	$Na_2SO_4$	"
Alumina adsorption	$Al_2O_3$	"
N,N-Dimethyl- formamide (DMF)	$HCON(CH_3)_2$	"
Chloroform	$CCl_3$	"
Methanol	$CH_3OH$	"
Petroleum ether	$(C_2H_5)_2O$	"
Hydrogen chloride	$HCl$	"
Sulfuric acid	$H_2SO_4$	"

Material	Formula	Manufacturer
Cupric chloride	$\text{CuCl}_2 \cdot 2\text{H}_2\text{O}$	Baker Chemical Co.
Silver nitrate	$\text{AgNO}_3$	"
Picric acid	$\text{C}_6\text{H}_3\text{N}_3\text{O}_7$	"
Cuprous chloride	$\text{CuCl}$	"
Silver acetate (AgAc)	$\text{AgCH}_3\text{COO}$	"
Chromium chloride	$\text{CrCl}_3 \cdot 6\text{H}_2\text{O}$	"
Stannous chloride	$\text{SnCl}_2 \cdot 2\text{H}_2\text{O}$	"
Magnesium sulfate	$\text{MgSO}_4$	"
Cadmium sulfate	$3\text{CdSO}_4 \cdot 8\text{H}_2\text{O}$	"
Cobalt carbonate	$\text{CoCO}_3$	"
Sodium chloride	$\text{NaCl}$	"
Sodium dichromate	$\text{Na}_2\text{Cr}_2\text{O}_7$	"
Molecular sieves	base: Alumina- silicate cation: calcium	"
Silver perchlorate	$\text{AgClO}_4$	Bio-Science Labs
Nickel "	$\text{Ni}(\text{ClO}_4)_2 \cdot 6\text{H}_2\text{O}$	"
Cobalt "	Co "	"
Zinc "	Zn "	"
Manganese "	Mn "	"
Tetrabutylammonium hydroxide (TB) (25% in methanol)	$(\text{C}_4\text{H}_9)_4\text{NOH}$	Eastman Kodak Co.
1,1,3,3-Tetramethyl -guanidine (TMG)	$(\text{CH}_3)_4\text{NC}(:\text{NH})\text{N}$	"
2,4-Pentanedione (2,4-PDO)	$(\text{CH}_3)_2\text{COCH}_2\text{CO}$	"
Ethylenediamine (EN)	$\text{C}_2\text{H}_8\text{N}_2$	"

Material	Formula	Manufacturer
Magnesium chloride	$\text{MgCl}_2 \cdot 6\text{H}_2\text{O}$	Allied Chemical Co.
Cadmium acetate ( $\text{CdAc}_2$ )	$\text{Cd}(\text{CH}_3\text{COO})_2 \cdot 2\text{H}_2\text{O}$	"
Magnesium perchlorate (anhydrous)	$\text{Mg}(\text{ClO}_4)_2$	G. Fredrick Smith Chemical Co.
Sodium perchlorate	$\text{NaClO}_4$	"
3-methyl-1-p- tolytriazene	$(\text{CH}_3)_2\text{C}_6\text{H}_4\text{N}=\text{NNH}$	Aldrich Chemical Co.
Argon (gas)	Ar	Aerco
Bilirubin (BR)	$\text{C}_{33}\text{H}_{36}\text{N}_4\text{O}_6$	Sigma Chemical Co.

## CHAPTER IV

## EXPERIMENTAL PROCEDURE AND RESULTS

A. Purification of DMF

DMF decomposes or hydrolyzes into dimethylamine, carbon monoxide, other amines and formic acid<sup>40</sup> within a few hours if exposed to normal light at room temperature. Reagent grade DMF has a large enough amount of these by-products in it that it must be purified in order to obtain good spectral or electroanalytical results. Even after purification and storage in the freezer in a container wrapped in foil, DMF shows signs of breakdown into its byproducts within as few as four days. Therefore the DMF used in this study was purified once a week, stored in a freezer in a foil wrapped container and returned to a stock solution to be redistilled when impurities appeared on spectra.

The purification process used was as follows: 1) tamer tabs were added to a two liter round bottom distillation flask to reduce foaming and bumping, 2) anhydrous  $\text{CuSO}_4$  was put into this flask to complex amines preventing their distillation, 3) 800 to 900 ml of DMF were added to the flask (if the flask was over half filled bumping problems usually arose), 4)  $\text{CaH}_2$  was added to the mixture to reduce the  $\text{H}_2\text{O}$  content of the purified DMF, 5)



the distillation was begun in an argon atmosphere under a vacuum of 4 to 9 torr and the temperature of the DMF vapors was maintained between 37 and 45° C by an electric heating mantle, 6) the first fraction of about one fifth of the initial volume was discarded, and 7) the middle fraction was collected and stored over molecular sieves in a freezer in a container wrapped in aluminum foil.

Control of the rate of distillation was accomplished by varying the argon flow and by varying the temperature and pressure. Control is very important because if the distillation proceeds too rapidly foaming, bumping, and loss of purity often results; if the distillation is run too slowly it could easily take over ten hours to obtain 400 to 500 ml of pure DMF. The preceding purification technique of DMF is a modified version of Szentirmay's<sup>41</sup> method. The addition of the use of CaH<sub>2</sub> and aluminum foil was suggested by Dr. R. C. Phillips. Glassware used for analytical work was cleaned in a hot dichromate solution for twenty minutes and rinsed with H<sub>2</sub>O.

## B. Standardization of the DMF System

In order to quantitatively remove protons from BR it was necessary to first standardize in DMF the two bases, TB and TMG, with an acid of well known behavior. Figures 2 and 4 show potentiometric titrations of picric acid with TB and TMG respectively and Figure 3 illustrates a first derivative plot used to more accurately find the inflection point of the TB titration curve.

It became of great interest to investigate the BR-proton system since it was observed both from this study and from Szentirmay's<sup>42</sup> that protons must be removed from BR in order for metal ions to form complexes with BR and since no complexation could be spectrally followed when optimum molar ratios of BR:base:metal ion were not closely approximated for each particular BR complex. Figure 5 indicates that four protons can be quantitatively removed from BR with TB. This titration of BR with TB was done three times all showing some indication of four protons coming off. Lee et al.<sup>11</sup> also used TB to titrate BR in DMF and stated that the first two equivalents of TB corresponded to the propionic protons and that the third and fourth equivalents involved the chromophore structure directly. They estimated  $pK_1$  and  $pK_2$  values to be 4.3 and 5.3 for the first two protons coming off. BRDME was also titrated with TB. Numerous breaks resulted, making interpretation very difficult.

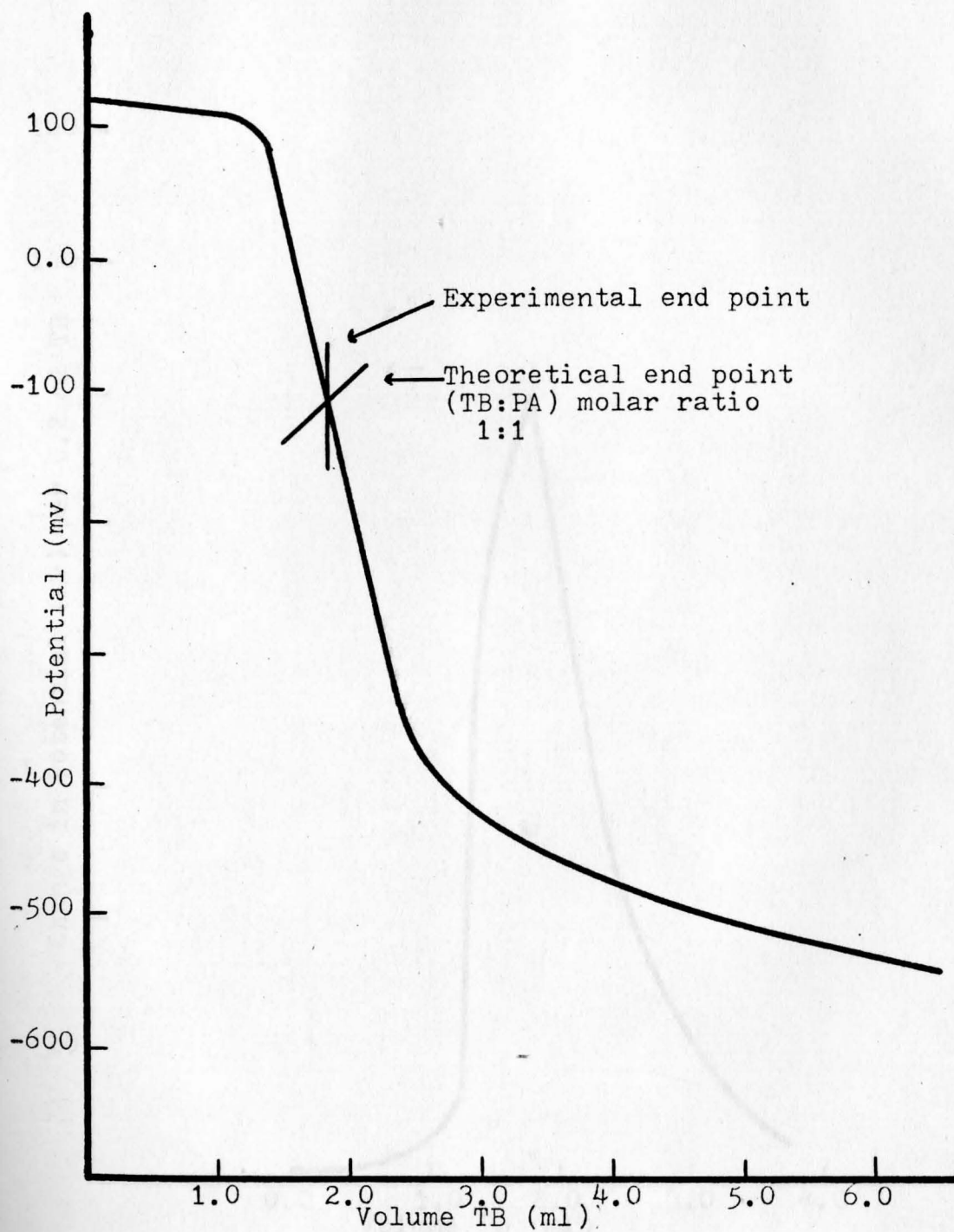


Figure 2. Potentiometric Titration of PA with TB.

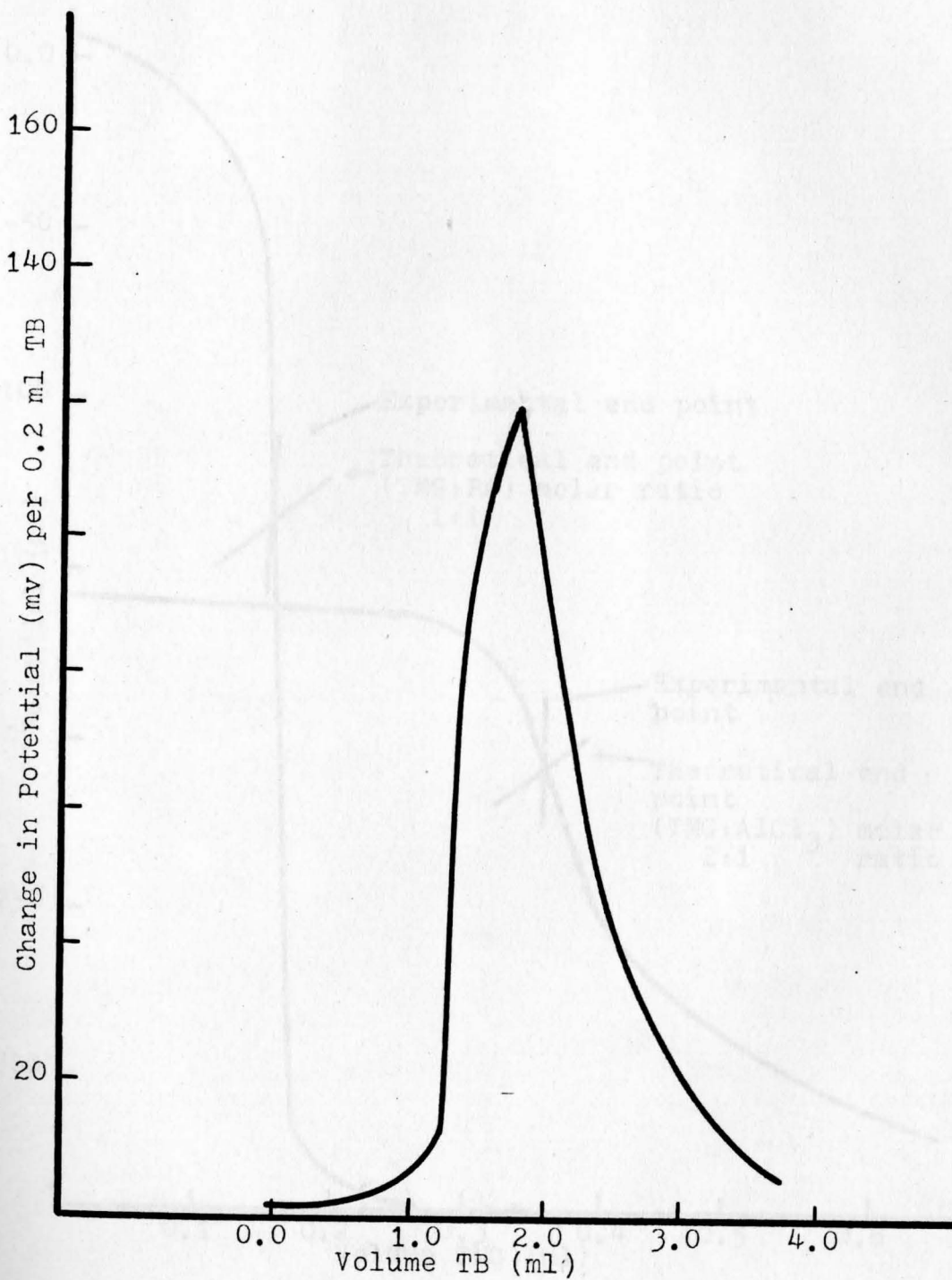


Figure 3. First Derivative Plot for the Titration of PA with TB.

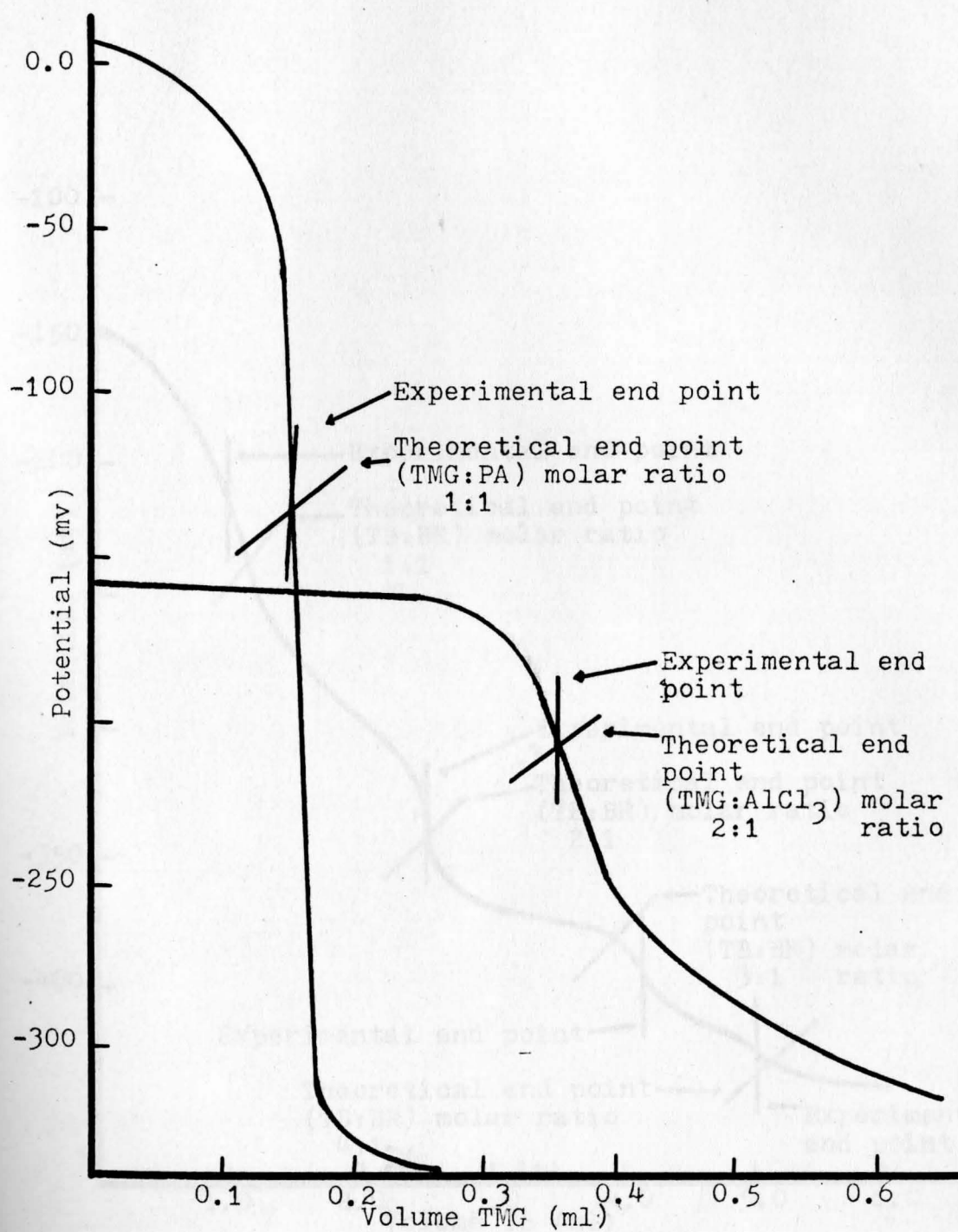


Figure 4. Potentiometric Titrations of PA and AlCl<sub>3</sub> with TMG.

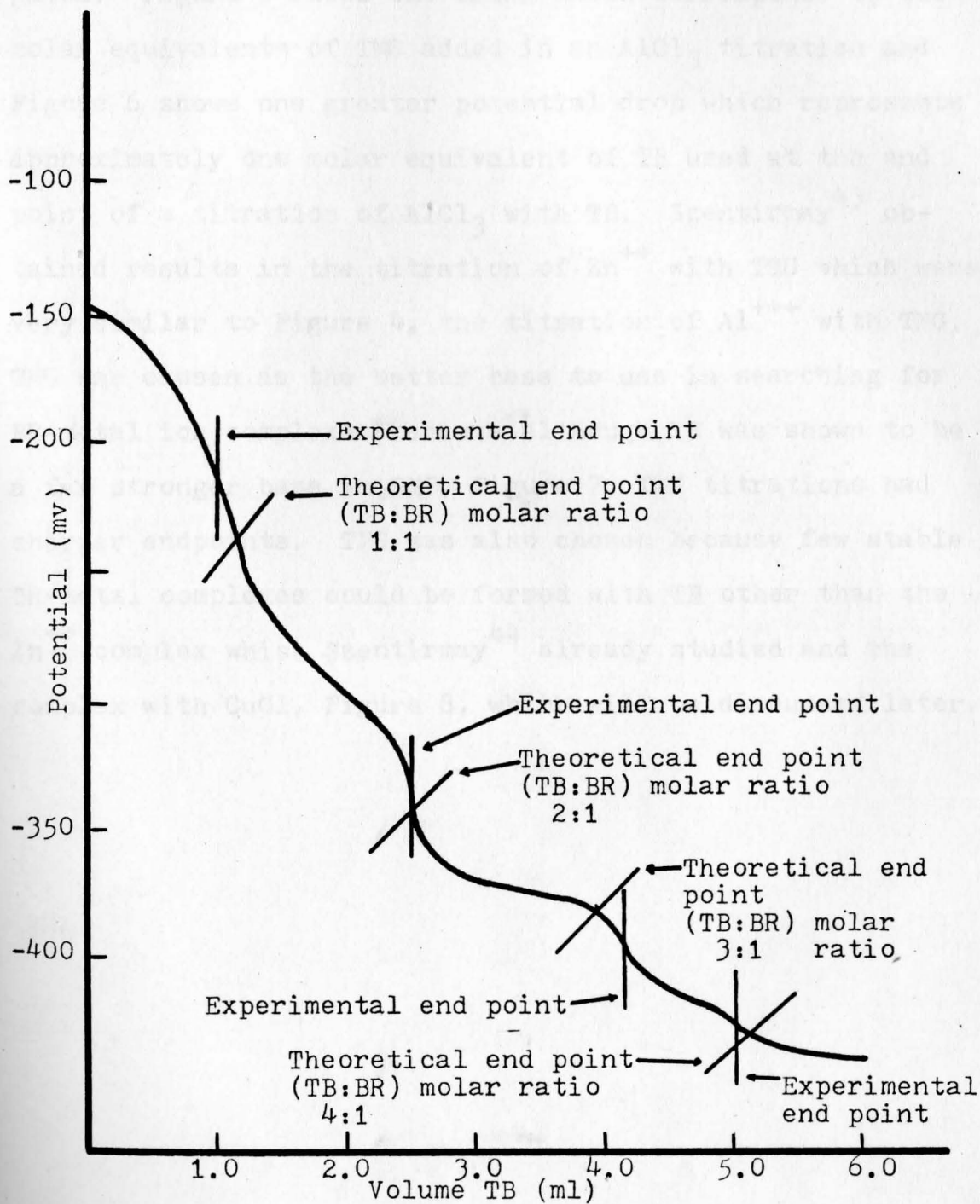


Figure 5. Potentiometric Titration of BR with TB.

Finally, since the metal ions which were reacted with BR are Lewis acids, some of them were also investigated. Figure 4 shows one break which corresponds to two molar equivalents of TMG added in an  $\text{AlCl}_3$  titration and Figure 6 shows one greater potential drop which represents approximately one molar equivalent of TB used at the endpoint of a titration of  $\text{AlCl}_3$  with TB. Szentirmay<sup>43</sup> obtained results in the titration of  $\text{Zn}^{++}$  with TMG which were very similar to Figure 4, the titration of  $\text{Al}^{+++}$  with TMG. TMG was chosen as the better base to use in searching for BR-metal ion complexes because although TB was shown to be a far stronger base in DMF, Figure 7, TMG titrations had sharper endpoints. TMG was also chosen because few stable BR-metal complexes could be formed with TB other than the  $\text{Zn}^{++}$  complex which Szentirmay<sup>44</sup> already studied and the complex with  $\text{CuCl}$ , Figure 8, which will be discussed later.

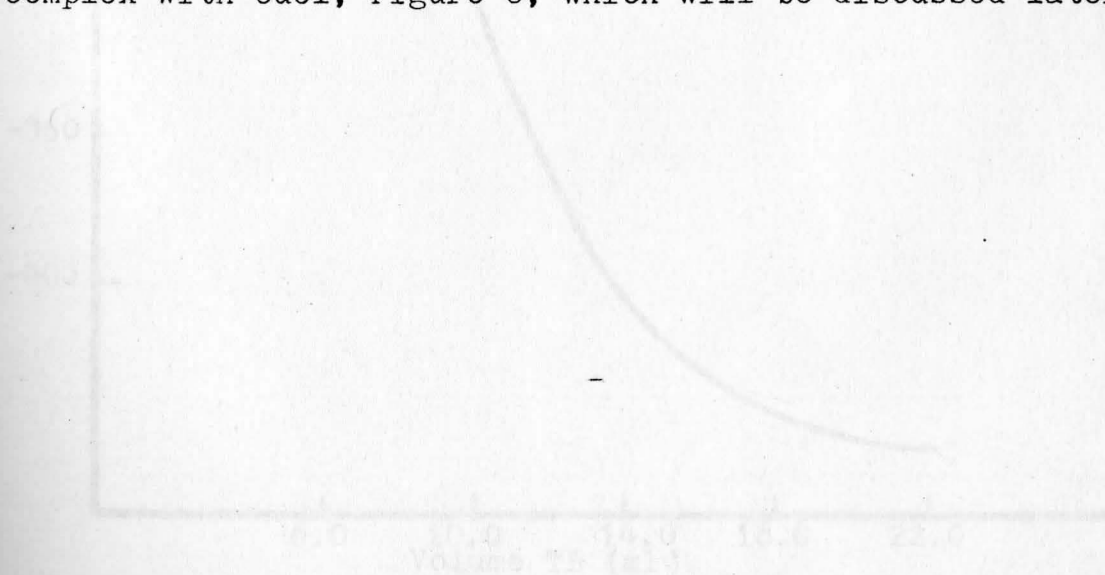


Figure 6. Potentiometric titration of  $\text{AlCl}_3$  with TB.

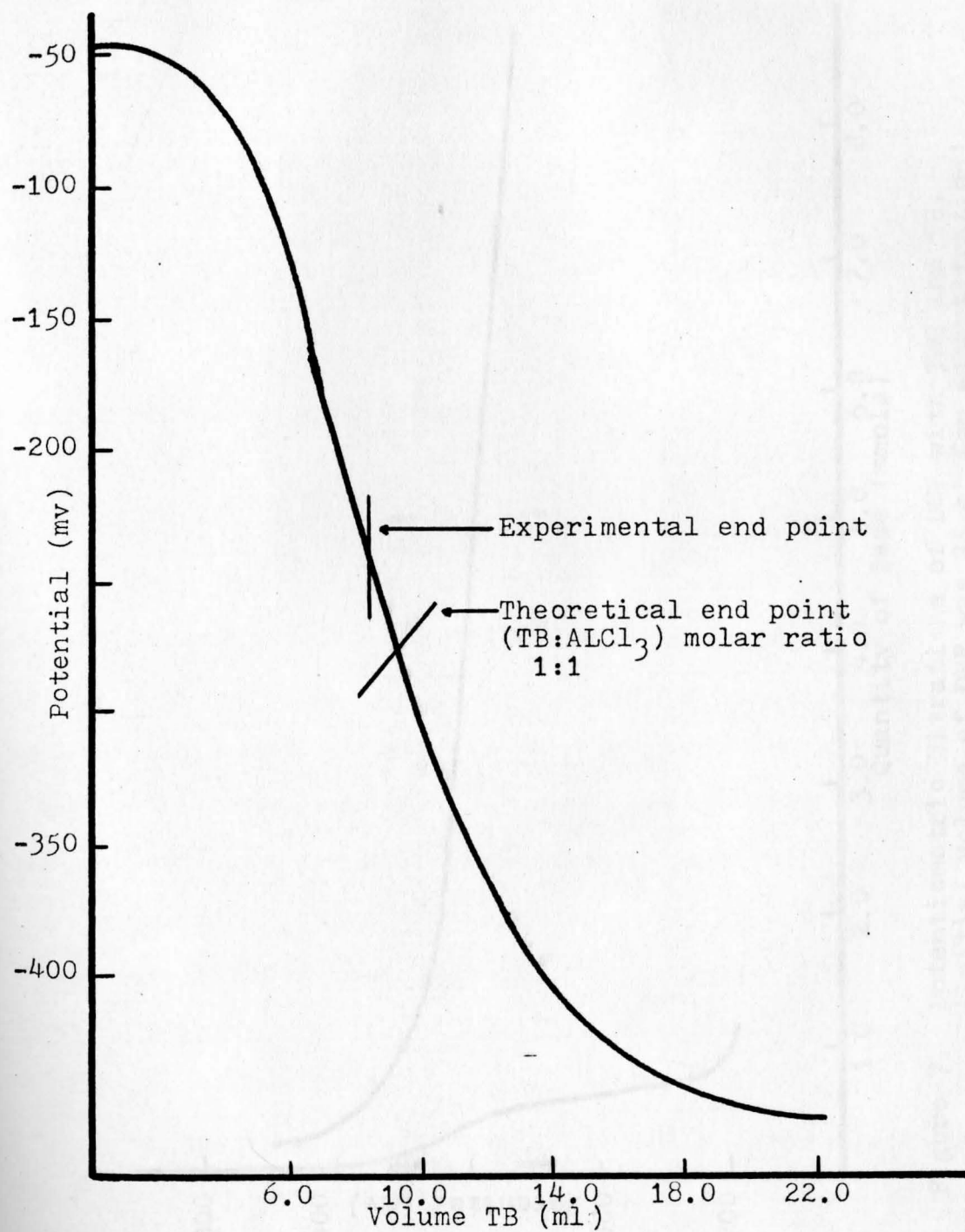


Figure 6. Potentiometric Titration of AlCl<sub>3</sub> with TB.



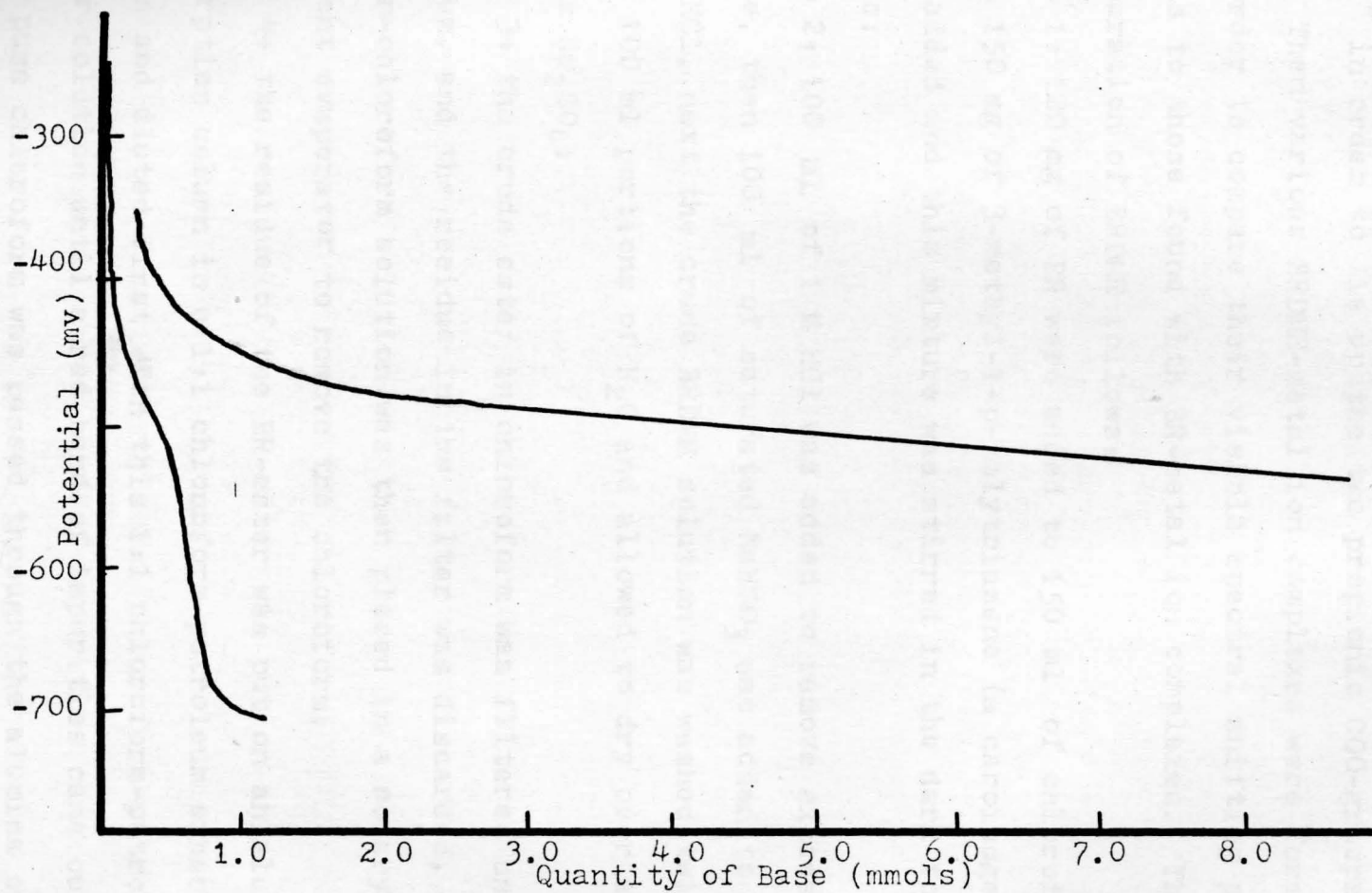


Figure 7. Potentiometric Titrations of DMF with TNG and TB.  
(Initial volume of DMF was 25 ml for each titration)

### C. Esterification of Bilirubin

BRDME was prepared by the method of Hutchinson et al.<sup>16</sup> in order to tie up the two propionic COO-groups of BR. Then various BRDME-metal ion complexes were formed in order to compare their visible spectral shifting patterns to those found with BR-metal ion complexes. The preparation of BRDME follows:

step 1: 120 mg of BR were added to 150 ml of chloroform, then 150 mg of 3-methyl-1-p-tolytriazene (a carcinogen) was added and this mixture was stirred in the dark for 12 hours;

step 2: 100 ml of 1 M HCl was added to remove excess triazene, then 100 ml of saturated NaHCO<sub>3</sub> was added to remove the HCl, next the crude BRDME solution was washed twice with 100 ml portions of H<sub>2</sub>O and allowed to dry over anhydrous Na<sub>2</sub>SO<sub>4</sub>;

step 3: the crude ester in chloroform was filtered under vacuum, and the residue in the filter was discarded, the ester-chloroform solution was then placed in a rotary solvent evaporator to remove the chloroform;

step 4: the residue of the BR-ester was put on an alumina absorption column in a 1:1 chloroform-petroleum ether solution and eluted first with this 1:1 chloroform-petroleum ether solution until a red band of impurities came out, then pure chloroform was passed through the alumina column to remove further impurities, finally a mixture of 20:1

chloroform-methanol solution was used to elute the remaining orange band of purified BRDME; step 5: the chloroform-methanol solvent was evaporated off using a rotary evaporator and the pure BRDME residue was stored in the freezer in a container wrapped in foil. BRDME appeared to be even more light sensitive than BR or DMF. Therefore it was always kept out of direct light. As long as a sharp 420-nm spectral peak, as in Figure 10, was obtained for this purified ester both in a chloroform and in a BRDME/TMG/DMF-solution similar to Mark's<sup>45</sup> BRDME peaks, the BR-ester was assumed to be pure enough for spectral work. One time when the normal 440-nm shoulder was too large it was decided that the ester should be re-eluted through the alumina column.

#### D. Qualitative Complexation of Bilirubin and Bilirubin Dimethyl Ester with Metal Salts

After many qualitative tests with BR/TB and various metal ions, only few stable complexes were able to be made. The  $ZnI_2$  one was of little further interest at this time because Szentirmay<sup>46</sup> had already done an extensive study on the Zn-BR system. Studies on one other, BR/TB/CuCl/TMG, were initiated. However, they were aborted because the 430-nm Cu-BR complex, Figure 8, could not be reversed back to the 450-nm BR-spectrum and because of the polarographic study done on copper in DMF described in section F of this chapter. So the next approach to the BR-metal ion

complexation problem was to go back and redo semiquantitative tests with various metal ions. This time however, TMG was used as the base and quick weighings of BR and the various metal ions were taken before each test. At first this procedure was very time consuming but after a number of runs and the use of Beers law to spectrally estimate the BR concentration, the process became much faster. Figures 9 and 10 show the visible spectra of BR and BRDME respectively under neutral, acidic and basic conditions. The differences in the absorbance peaks of the various forms of BR could very likely be due to differences in the intramolecular hydrogen bonding and the amount of electron movement through BR's pyrrole rings. Neutral BR probably has hydrogen bonding as illustrated by Manitto and Monti,<sup>22</sup> drawn in Figure 25. Kuenzle et al.<sup>23</sup> proposed similar intramolecular hydrogen bonding from BR's COO-groups to the nitrogens and oxygens of the outside rings only. Either form of hydrogen bonding should help maintain the planarity of BR's four pyrrole rings. If BR's two COO-groups are methylated, BR's intramolecular hydrogen bonding could very well be broken, as illustrated by Kuenzle et al.,<sup>23</sup> resulting in some loss of planarity among BR's four pyrrole rings. Loss of planarity would hinder electron movement between rings. This could explain BRDME's absorbance peak occurring at a shorter wavelength than BR's peak. Basic BR probably has two protons removed at sites 5 and 6 of

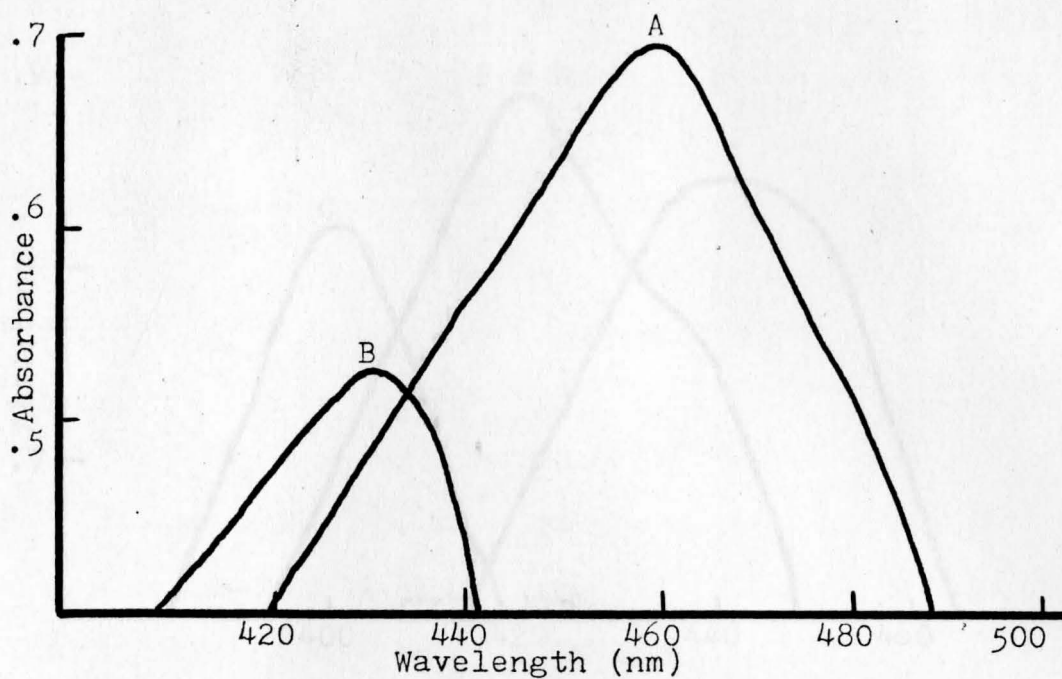


Figure 8. Visible Spectra of BR/TB/CuCl/DMF.

A- BR/TB/DMF  
 B- BR/TB/Cu<sup>+</sup>/DMF  
 1 : 2 : 2 molar ratio

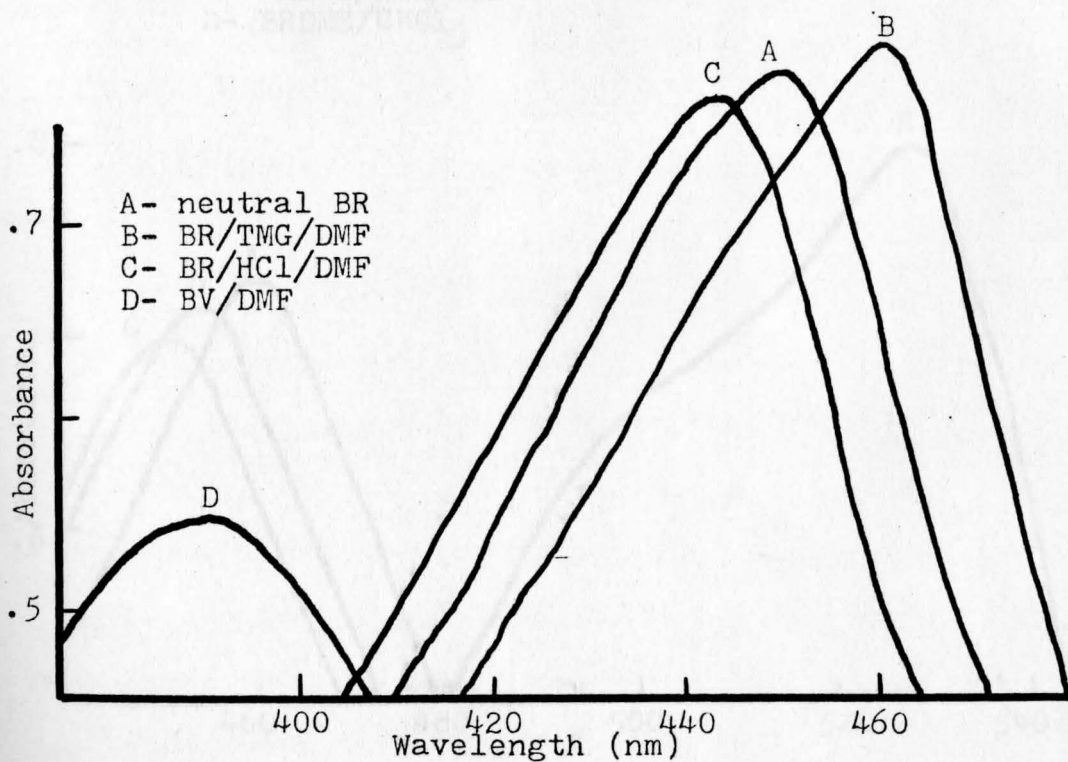


Figure 9. Visible Spectra of Acid-Base Behavior of BR in DMF.

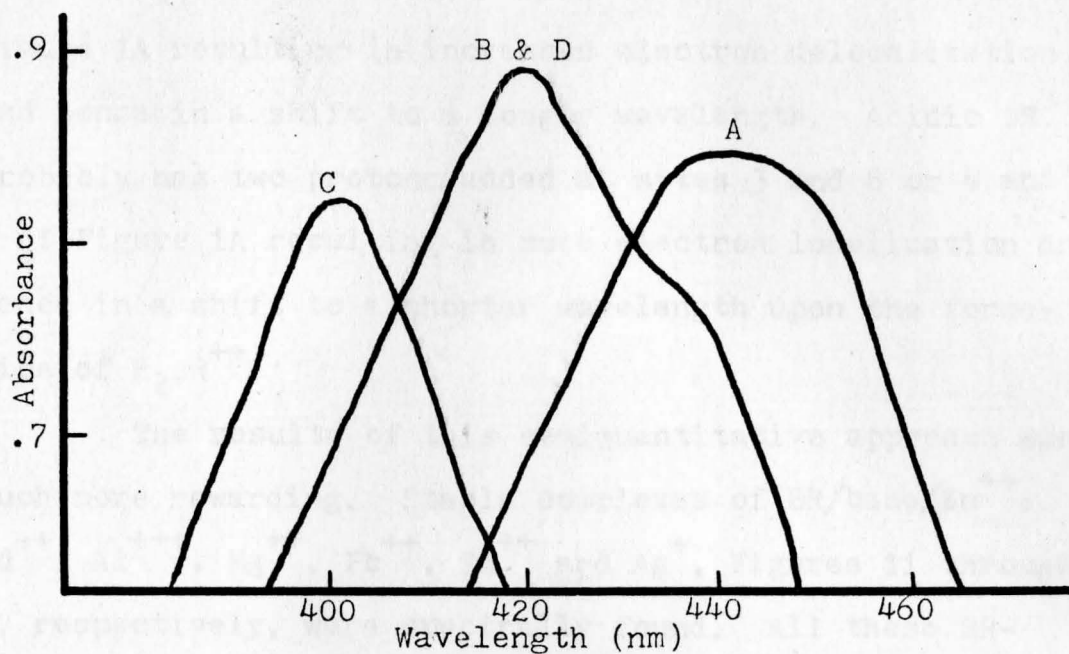


Figure 10. Visible Spectra of Acid-Base Behavior of BRDME in DMF and BRDME in  $\text{CHCl}_3$ .  
 A- neutral BRDME/DMF  
 B- BRDME/TMG/DMF  
 C- BRDME/HCl/DMF  
 D- BRDME/ $\text{CHCl}_3$

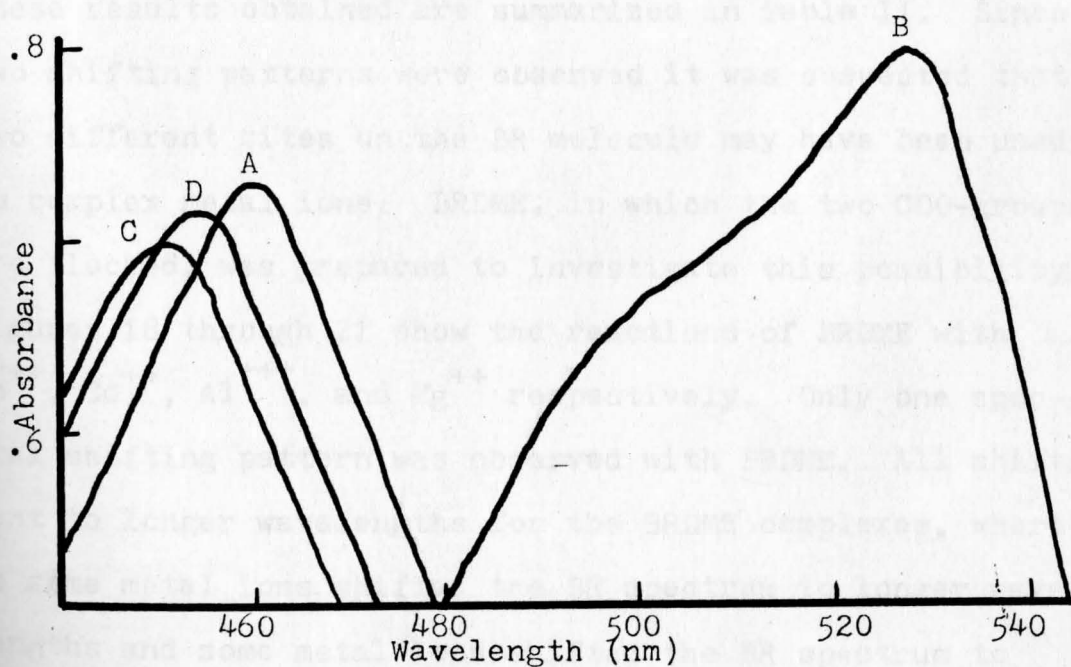


Figure 11. Visible Spectra of BR/TMG/ $\text{ZnI}_2$ /DMF.  
 A- BR/TMG/DMF  
 B- BR/TMG/ $\text{Zn}^{++}$ /DMF  
 C- B + 2,4-PDO  
 D- B + EN

Figure 1A resulting in increased electron delocalization and hence in a shift to a longer wavelength. Acidic BR probably has two protons added at sites 3 and 8 or 4 and 7 of Figure 1A resulting in more electron localization and hence in a shift to a shorter wavelength upon the formation of  $H_2BR^{++}$ .

The results of this semiquantitative approach were much more rewarding. Stable complexes of BR/base/ $Zn^{++}$ ,  $Cd^{++}$ ,  $Al^{+++}$ ,  $Mg^{++}$ ,  $Pb^{++}$ ,  $Sn^{++}$  and  $Ag^+$ , Figures 11 through 17 respectively, were spectrally found. All these BR-metal ion complexes immediately shifted the BR 450-nm peak and all could be reversed back to the 450-nm BR spectrum. This indicates that these metal ions did in fact complex the BR molecule without altering the structure of BR. These results obtained are summarized in Table II. Since two shifting patterns were observed it was suspected that two different sites on the BR molecule may have been used to complex metal ions. BRDME, in which the two COO-groups are blocked, was prepared to investigate this possibility. Figures 18 through 21 show the reactions of BRDME with  $Zn^{++}$ ,  $Cd^{++}$ ,  $Al^{+++}$ , and  $Mg^{++}$  respectively. Only one spectral shifting pattern was observed with BRDME. All shifts went to longer wavelengths for the BRDME complexes, whereas some metal ions shifted the BR spectrum to longer wavelengths and some metal ions shifted the BR spectrum to shorter wavelengths. Therefore it is here proposed that

TABLE II  
CLASSIFICATION OF BR REACTIONS IN DMF

The Reversible Al-type		The Reversible Zn-type	
Metal Salt	Peak (nm)	Metal Salt	Peak (nm)
AlCl <sub>3</sub>	420	ZnI <sub>2</sub>	520
CdCl <sub>2</sub> ·2.5H <sub>2</sub> O	428	AlCl <sub>3</sub> ·6H <sub>2</sub> O	458
PbCl <sub>2</sub>	420	3CdSO <sub>4</sub> ·8H <sub>2</sub> O	460
AgNO <sub>3</sub>	416	NiCl <sub>2</sub> ·6H <sub>2</sub> O	514
SnCl <sub>2</sub> ·2H <sub>2</sub> O	417	CdAc <sub>2</sub> ·2H <sub>2</sub> O	533
MgSO <sub>4</sub>	424	Zn(ClO <sub>4</sub> ) <sub>2</sub> ·6H <sub>2</sub> O	521
CoCO <sub>3</sub>	428		
CoCl <sub>2</sub> ·6H <sub>2</sub> O	418		
AgAc	418		
MgCl <sub>2</sub> ·6H <sub>2</sub> O	414		
The Non-reversible Cu-type		The Slow Equilibrium Fe-type	
CuCl	430	FeSO <sub>4</sub> ·7H <sub>2</sub> O	442-472
CuCl <sub>2</sub>	379	CrCl <sub>3</sub> ·6H <sub>2</sub> O	400-440
AgClO <sub>4</sub>	424	Ni(ClO <sub>4</sub> ) <sub>2</sub> ·6H <sub>2</sub> O	420-435
Mn(ClO <sub>4</sub> ) <sub>2</sub> ·6H <sub>2</sub> O	338		
Co(ClO <sub>4</sub> ) <sub>2</sub> ·6H <sub>2</sub> O	392		
Mg(ClO <sub>4</sub> ) <sub>2</sub>	420		
NiAc <sub>2</sub> ·4H <sub>2</sub> O	374		
CoAc <sub>2</sub> ·4H <sub>2</sub> O	340		
NiCO <sub>3</sub>	432		



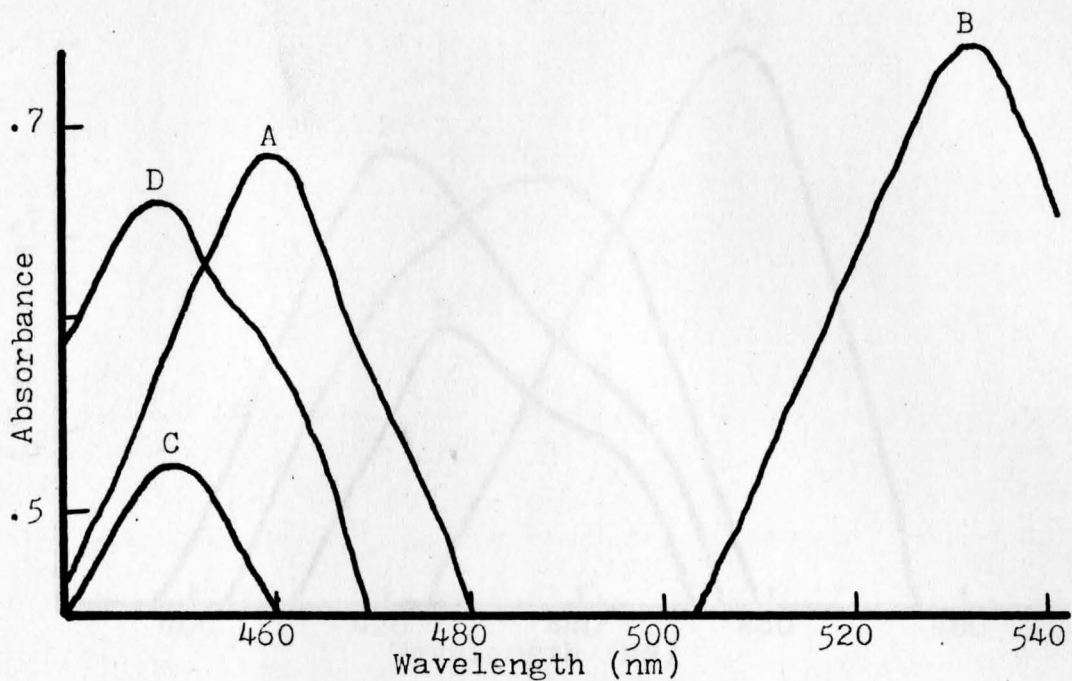


Figure 12. Visible Spectra of BR/TMG/CdAc<sub>2</sub>.2H<sub>2</sub>O/DMF.  
 A- BR/TMG/DMF  
 B- BR/TMG/Cd<sup>++</sup>/DMF  
 C- B + 2,4-PDO  
 D- B + EN

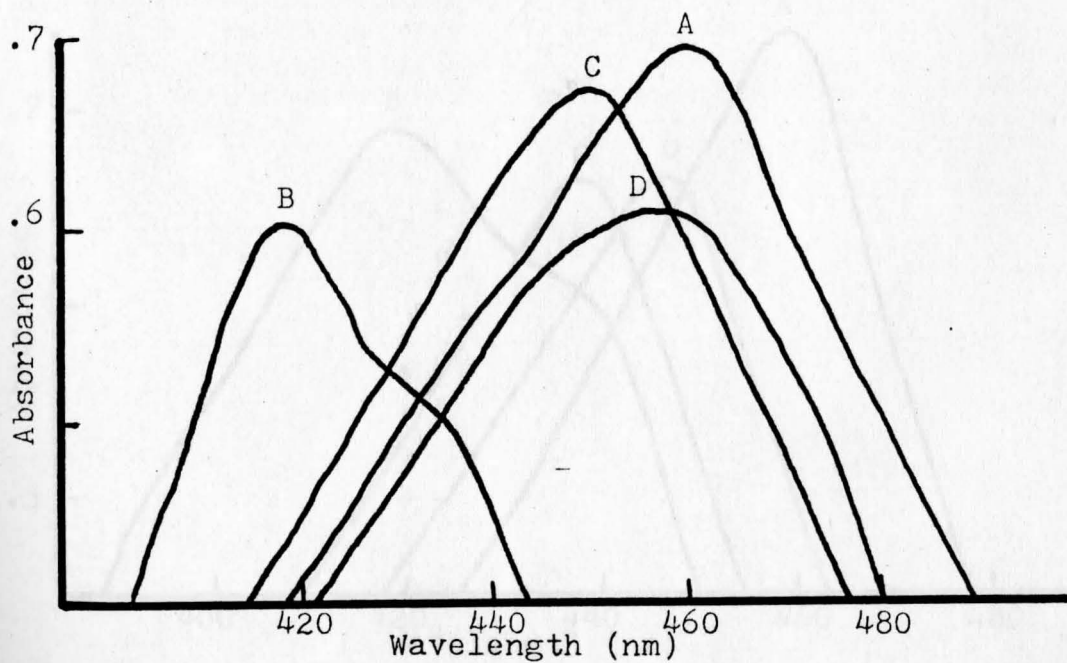


Figure 13. Visible Spectra of BR/TMG/AlCl<sub>3</sub>/DMF.  
 A- BR/TMG/DMF  
 B- BR/TMG/Al<sup>+++</sup>/DMF  
 C- B + 2,4-PDO  
 D- B + EN

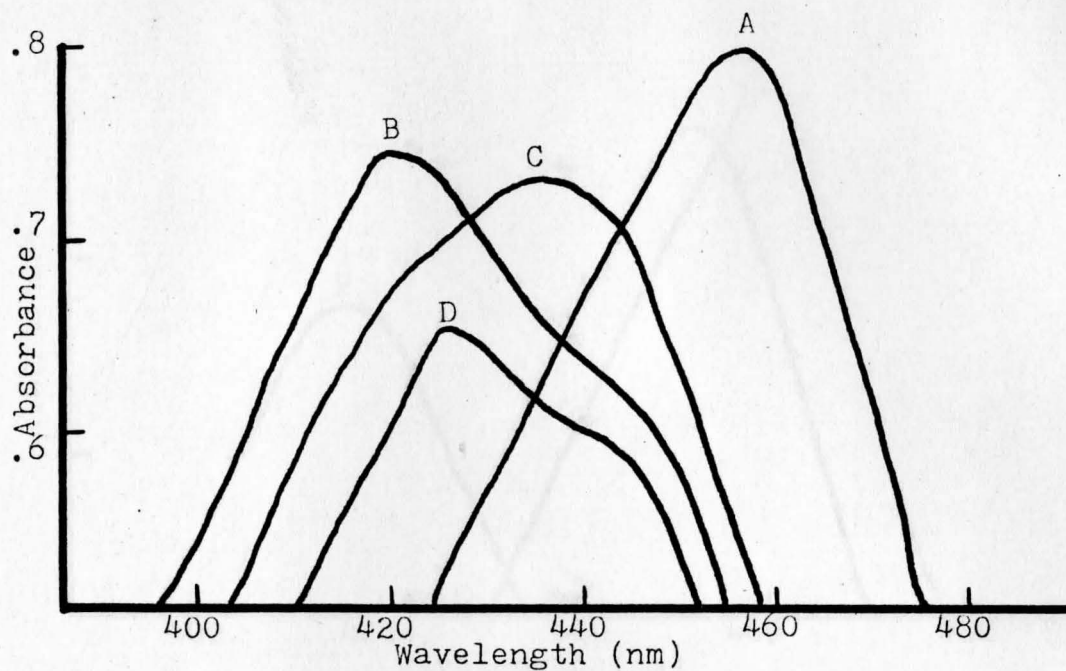


Figure 14. Visible Spectra of BR/TMG/MgCl<sub>2</sub>·6H<sub>2</sub>O/DMF.  
 A- BR/TMG/DMF  
 B- BR/TMG/Mg<sup>++</sup>/DMF  
 C- B + 2,4-PDO  
 D- B + EN

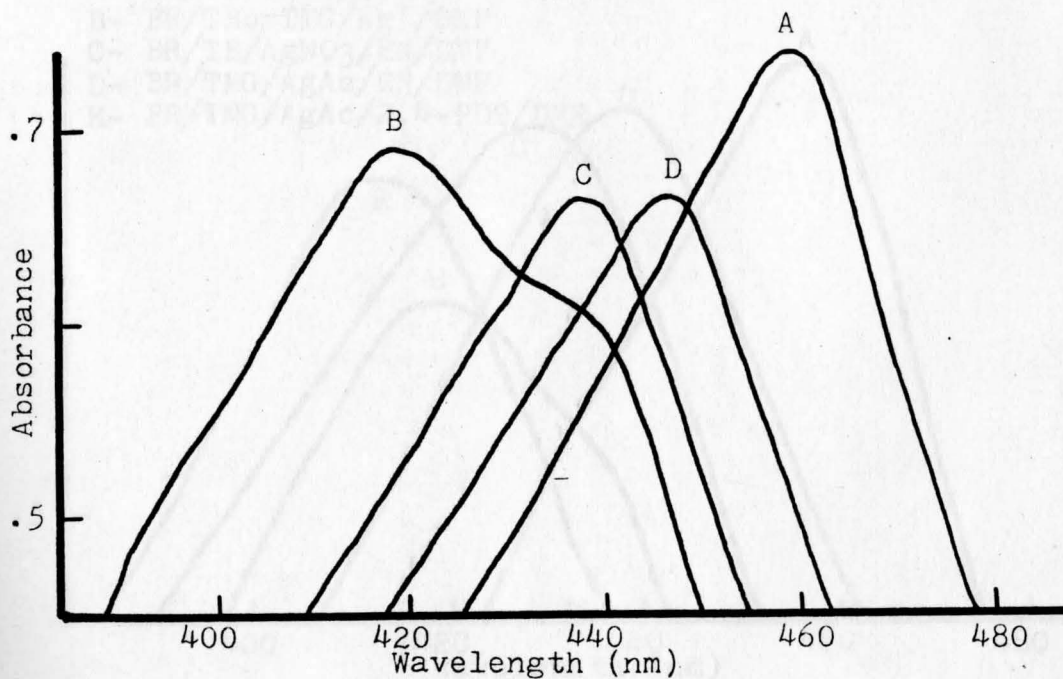


Figure 15. Visible Spectra of BR/TB/PbCl<sub>2</sub>/DMF.  
 A- BR/TB/DMF  
 B- BR/TB/Pb<sup>++</sup>/DMF  
 C- B + 2,4-PDO  
 D- B + EN

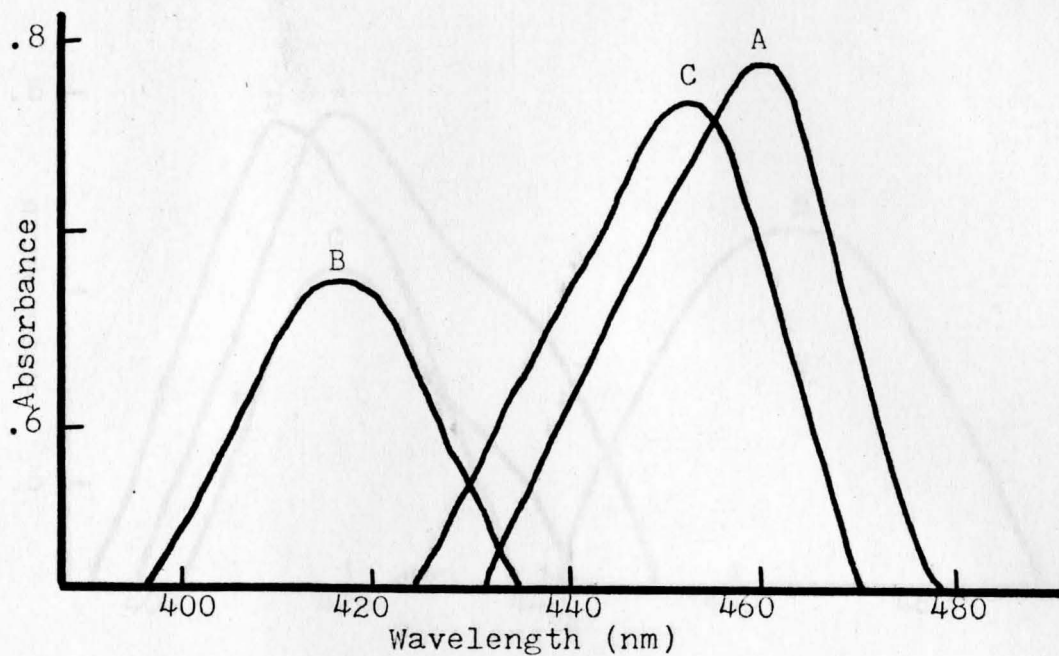


Figure 16. Visible Spectra of BR/TB/SnCl<sub>2</sub>·2H<sub>2</sub>O/DMF.

- A- BR/TB/DMF
- B- BR/TB/Sn<sup>++</sup>/DMF
- C- B + EN

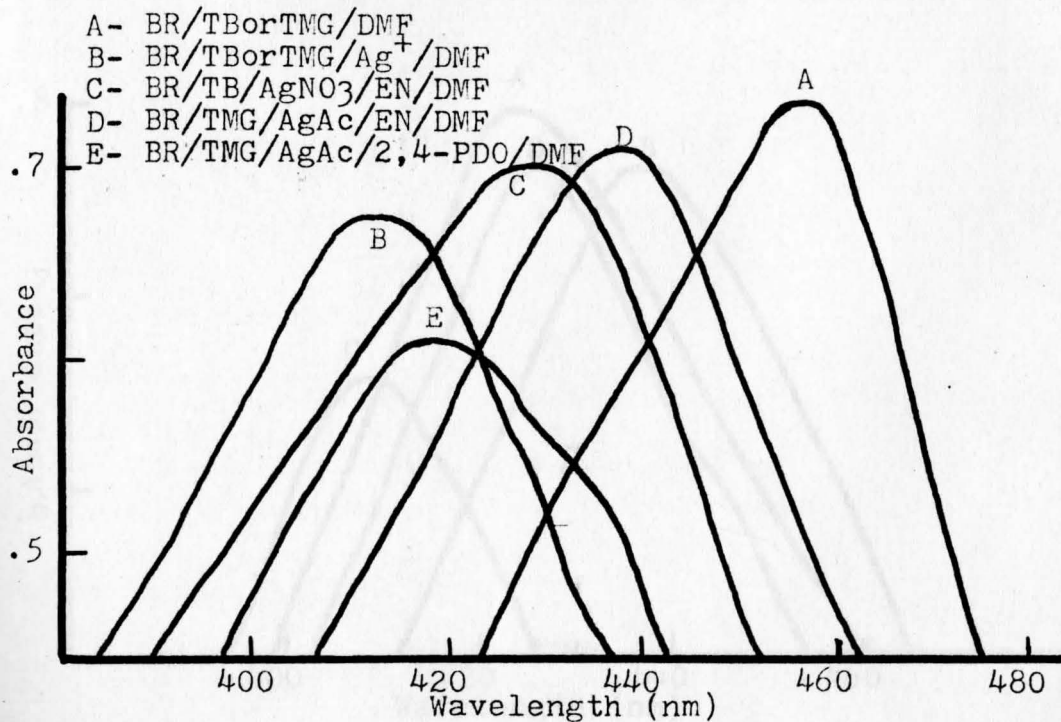


Figure 17. Visible Spectra of BR/TB/AgNO<sub>3</sub>/DMF and BR/TMG/AgAc/DMF.

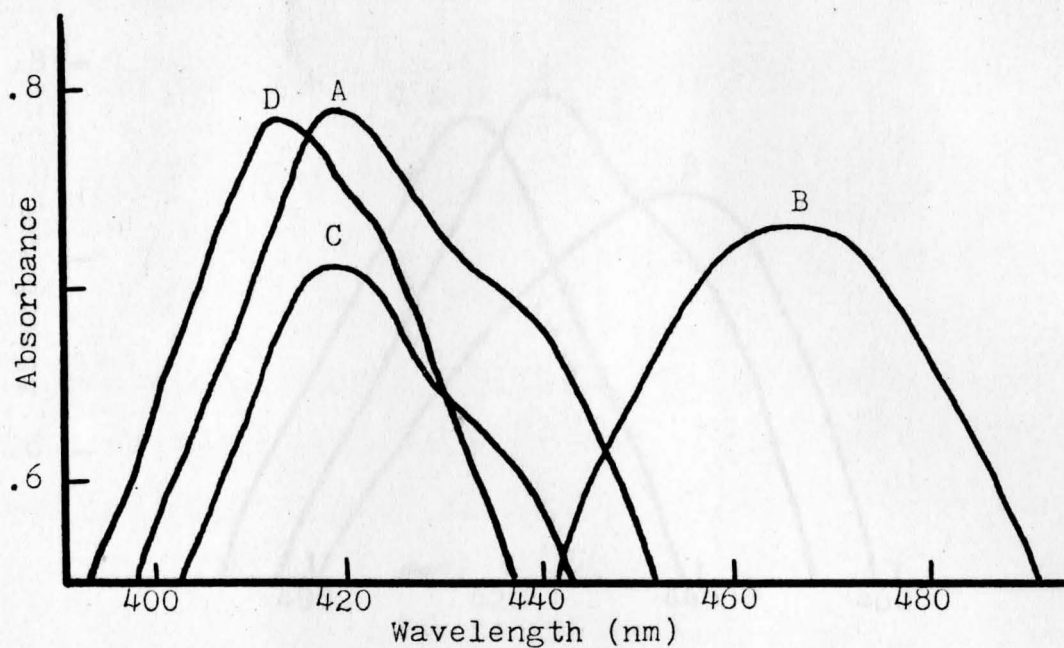


Figure 18. Visible Spectra of BRDME/TMG/ $ZnI_2$ /DMF.  
 A- BRDME/TMG/DMF  
 B- BRDME/TMG/ $Zn^{++}$ /DMF  
 C- B + 2,4-PDO  
 D- B + EN

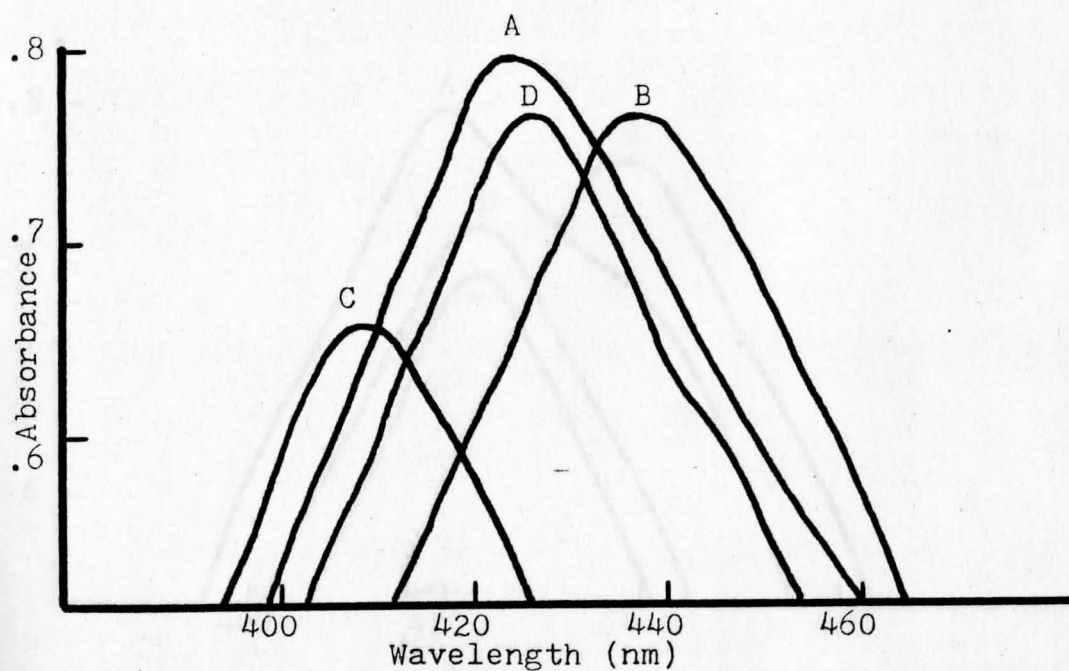


Figure 19. Visible Spectra of BRDME/TMG/ $CdAc_2 \cdot 2H_2O$ /DMF.  
 A- BRDME/TMG/DMG  
 B- BRDME/TMG/ $Cd^{++}$ /DMF  
 C- B + 2,4-PDO  
 D- B + EN

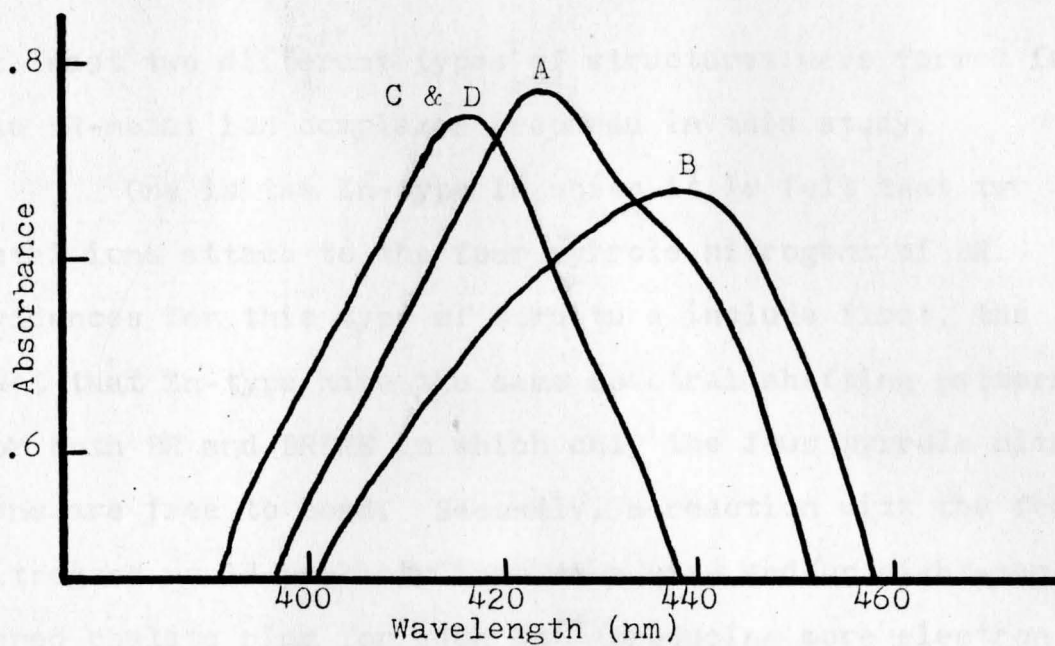


Figure 20. Visible Spectra of BRDME/TMG/AlCl<sub>3</sub>/DMF.

- A- BRDME/TMG/DMF  
 B- BRDME/TMG/Al<sup>+++</sup>/DMF  
 C- B + 2,4-PDO  
 D- B + EN

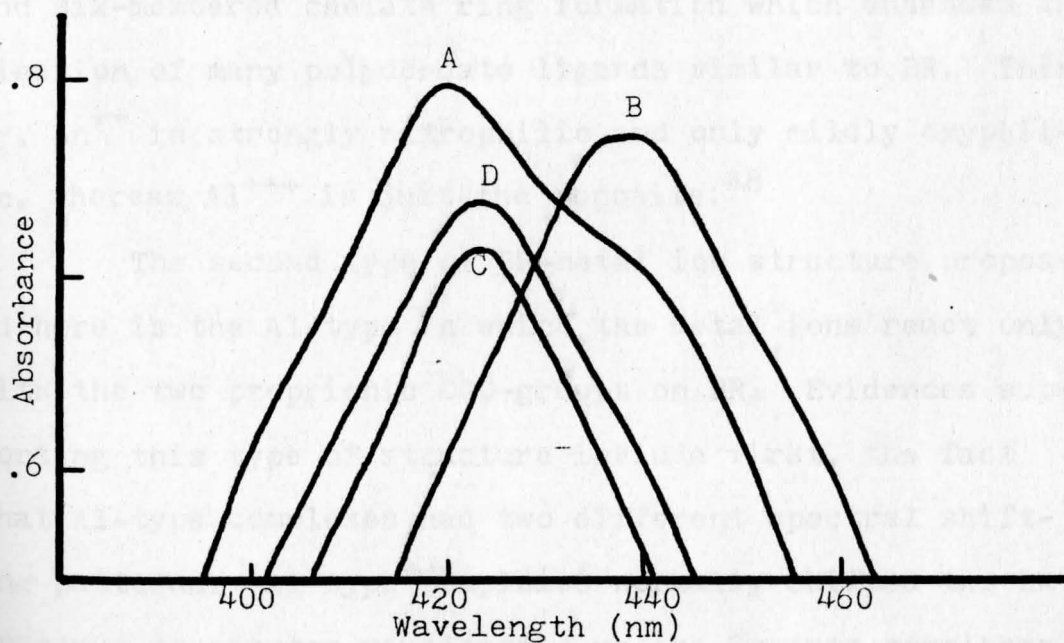


Figure 21. Visible Spectra of BRDME/TMG/MgCl<sub>2</sub>·6H<sub>2</sub>O/DMF.

- A- BRDME/TMG/DMF  
 B- BRDME/TMG/Mg<sup>++</sup>/DMF  
 C- B + 2,4-PDO  
 D- B + EN

at least two different types of structures were formed for the BR-metal ion complexes prepared in this study.

One is the Zn-type in which it is felt that two metal ions attach to the four pyrrole nitrogens of BR. Evidences for this type of structure include first, the fact that Zn-type have the same spectral shifting patterns for both BR and BRDME in which only the four pyrrole nitrogens are free to bond. Secondly, a reaction with the four nitrogens would probably involve a six- and/or eight-membered chelate ring for each  $Zn^{++}$  producing more electron delocalization and thus greater molecular stability which corresponds to absorbance peaks at longer wavelengths as was seen here for Zn-type BR complexes. Bailar<sup>47</sup> stated that the  $Zn^{++}$  has an ideal size and charge for stable five- and six-membered chelate ring formation which enhances the ligation of many polydentate ligands similar to BR. Thirdly,  $Zn^{++}$  is strongly nitrophilic and only mildly oxyphilic, whereas  $Al^{+++}$  is just the opposite.<sup>48</sup>

The second type of BR-metal ion structure proposed here is the Al-type in which the metal ions react only with the two proprionic COO-groups on BR. Evidences supporting this type of structure include first, the fact that Al-type complexes had two different spectral shifting patterns. Al-type complexes normally shifted the BR spectrum to shorter wavelengths unlike Zn-type complexes. When the two COO-groups on BR were blocked and the only likely sites free were the four nitrogens on the pyrrole

rings, formation of Al-type complexes did result in shifts of the BRDME spectrum to longer wavelengths as in the Zn-type. Secondly, Al-type shifts of the BR spectrum to shorter wavelengths paralleled BRDME shifts to shorter wavelengths. This indicates that  $Al^{+++}$  binds BR's two COO-groups in a manner similar to the way the methyl groups bind BR in the formation of BRDME described on page 34. Intramolecular hydrogen bonding is lost resulting in loss of planarity and thus in hindrance to electron movement in BR's pyrrole rings. Thirdly, the small trivalent  $Al^{+++}$  has a higher ionic potential than  $Zn^{++}$  to be a good candidate for the formation of stable chelate rings with the four pyrrole nitrogens of BR. And finally, when coordinating four or six ligands,  $Al^{+++}$  must form electron deficient tetrahedral or octahedral complexes. No  $Al^{+++}$  tetrahedral and only a few octahedral electron deficient chelate rings have been reported.<sup>49</sup>

Figures 22, 23 and 24 show likely structures for the stable BR-metal ion complexes found in this study. Hutchinson et al.<sup>13</sup> and Kuenzle et al.<sup>14</sup> have proposed BR-metal ion structures similar to the Zn-type deduced from this study. No structure was able to be found in the literature for a BR complex with a metal ion like the structure proposed in Figure 24. The Kuenzle et al.<sup>14</sup> structure for  $Sm_2$ -BR has possible drawbacks. First, eight-membered chelate rings are rare.<sup>50</sup> Second,  $Sm^{+++}$  appears to be an unlikely metal ion for a chelate structures such as

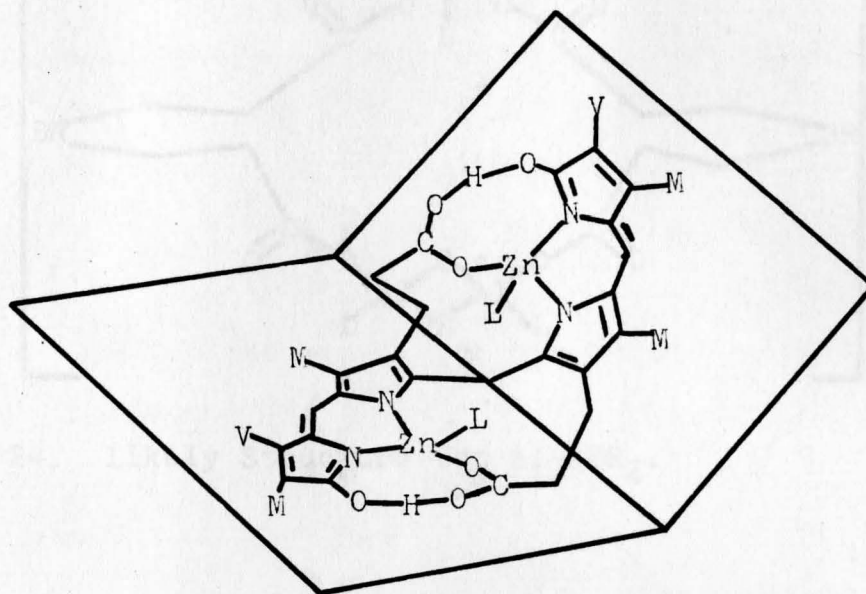


Figure 22. Likely Structure for  $Zn_2$ -BR.  
(L represents any ligand)

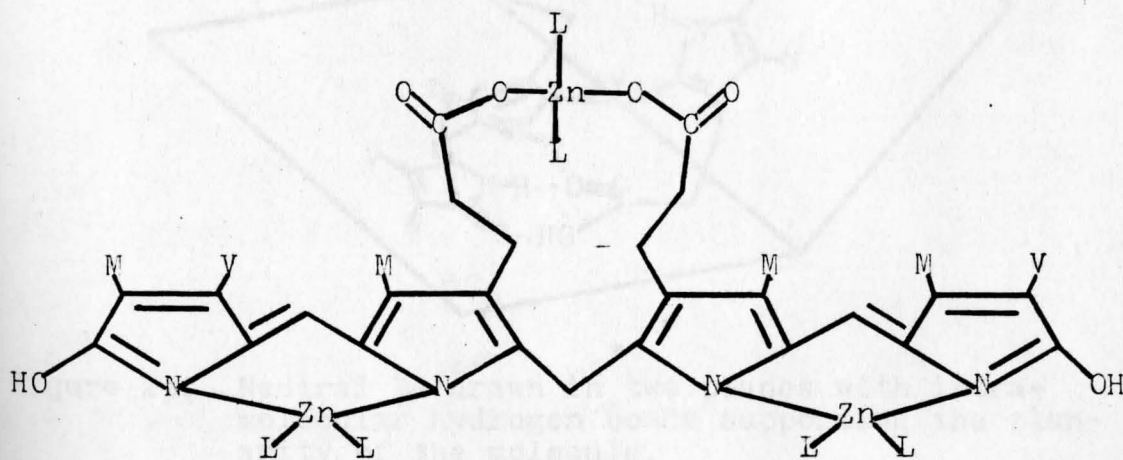


Figure 23. Likely Structure for  $Zn_3$ -BR.



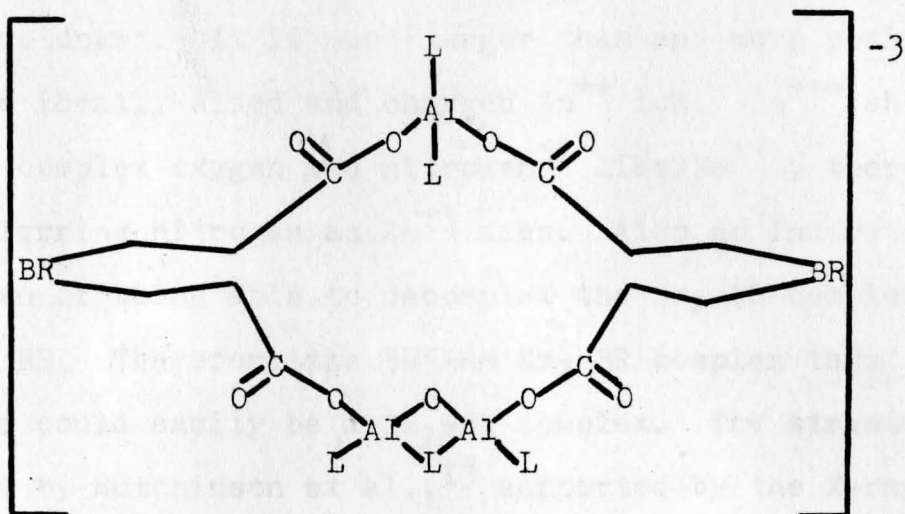


Figure 24. Likely Structure for  $Al_3-BR_2$ .

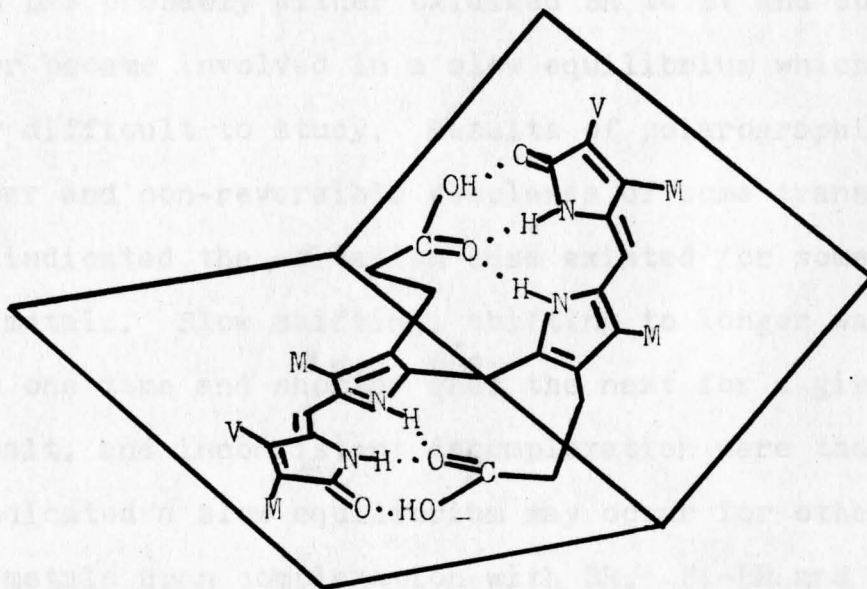


Figure 25. Neutral BR drawn in two planes with intramolecular hydrogen bonds supporting the planarity of the molecule.

they have drawn. It is much larger than and more positive than the ideally sized and charged  $Zn^{++}$  ion.  $Sm^{+++}$  should equally complex oxygen and nitrogen<sup>51</sup> like  $Fe^{++}$ , thereby not preferring nitrogen as  $Zn^{++}$  does. Also no indication was given of being able to decomplex the  $Sm_2$ -BR complex back to BR. Therefore the 395-nm  $Sm_2$ -BR complex they reported could easily be a  $Sm_2$ -BV complex. The structure proposed by Hutchinson et al.,<sup>13</sup> supported by the X-ray crystallography they performed, and having two six-membered stabilizing chelate rings with a third  $Zn^{++}$  bound to the two COO-groups of BR agrees well with the conclusions drawn from this study for Zn-type structures.

The first-period transition metals which were soluble in DMF probably either oxidized BR to BV and complexed BV or became involved in a slow equilibrium which would be very difficult to study. Results of polarographic work on copper and non-reversible complexes of some transition metals indicated the oxidation case existed for some transition metals. Slow shifting, shifting to longer wavelengths one time and shorter ones the next for a given metal salt, and inconsistent decomplexation were the signs that indicated a slow equilibrium may occur for other transition metals upon complexation with BR. Fe-BR and Cr-BR complexes were the two outstanding examples of the later case. Cu-type was the name given in Table II to describe the oxidation case and Fe-type was the name used to describe the slow equilibrium case. These Fe-type complexes

of BR may contain metal ions too large to form the stabilizing chelate rings for which  $Zn^{++}$  has been cited to have an ideal size. Also most of the larger transition metals complex oxygen and nitrogen equally well.<sup>52</sup> So transition metal ions which form Fe-type complexes of BR could be involved in a slow equilibrium between BR's oxygens and nitrogens.

E. Quantitative Complexation of Bilirubin and Bilirubin Dimethyl Ester with Zinc and Aluminum Salts

Spectrophotometric titrations were run on BR and BRDME with  $ZnI_2$  and  $AlCl_3$  both in order to follow the formation of these complexes in a step by step sequence and to determine the optimum molar ratios of BR or BRDME:TMG: $Al^{+++}$  or  $Zn^{++}$  complexes. Figures 26 through 29 show the results of the titrations. Szentirmay<sup>53</sup> obtained an optimum molar ratio of 1:8:2 at 540 nm for BR:TMG: $Zn^{++}$ . Figure 26 reproduced three times shows an optimum molar ratio of 1:8:3 for BR:TMG: $ZnI_2$  at 520 nm. These two sets of results probably differ because of the source of the  $Zn^{++}$  ion. Szentirmay generated his  $Zn^{++}$  electrochemically and the metal salt,  $ZnI_2$ , was the source of the  $Zn^{++}$  for the titration shown in Figure 26. This indicates that the nature of the other ligands or anions on the complexing metal ions affect complexation. Table II on page 38 shows Al and Cd salts differing only in the anions, forming both Zn-type and Al-type BR complexes.

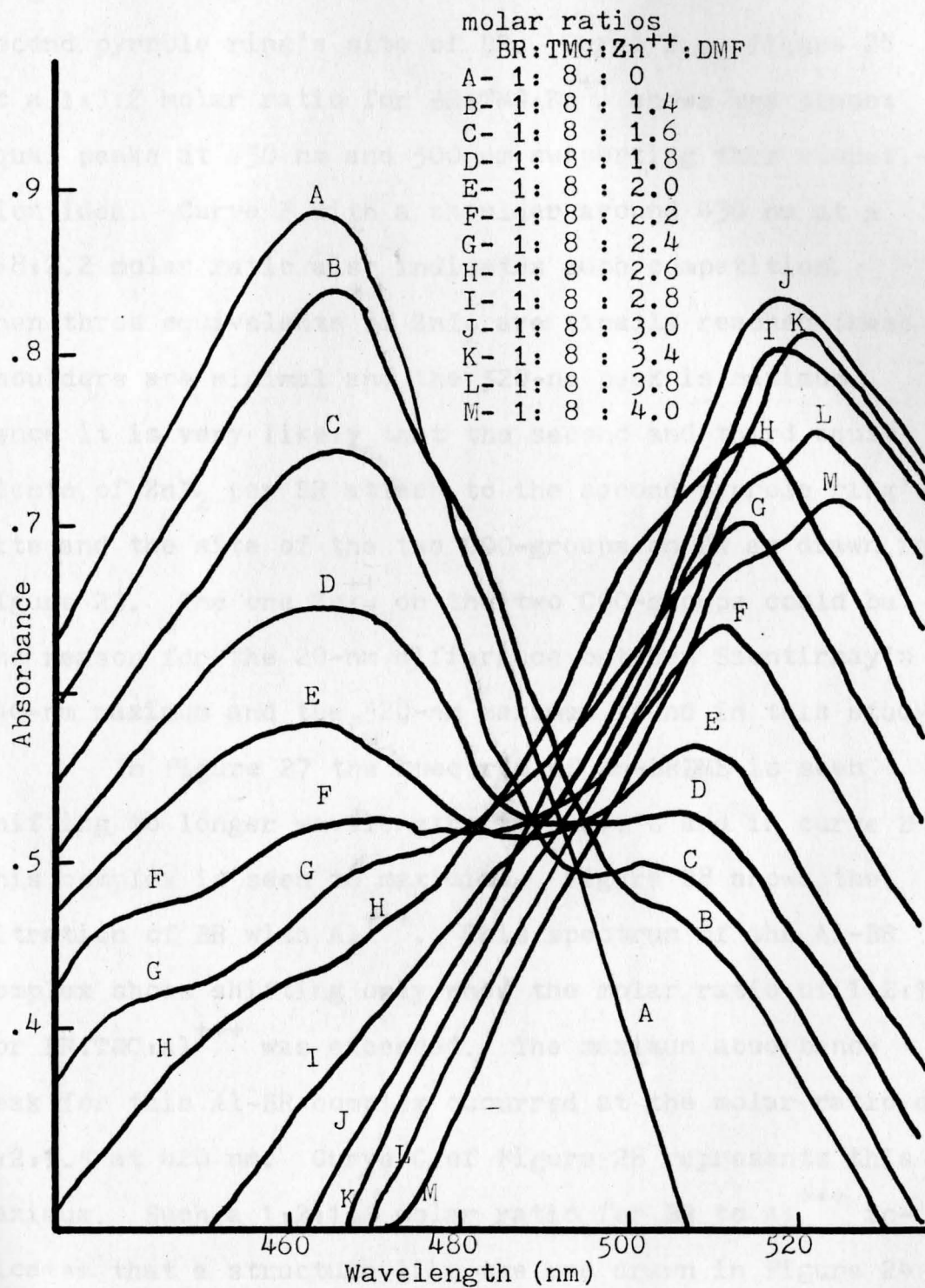


Figure 26. Spectrophotometric Titration of BR/TMG with ZnI<sub>2</sub>/DMF.

The second attaching  $Zn^{++}$  of this study could be caught in a competition between the COO-groups and the second pyrrole ring's site of BR. Curve E on Figure 26 at a 1:8:2 molar ratio for BR:TMG: $Zn^{++}$  shows two almost equal peaks at 450 nm and 500 nm supporting this competition idea. Curve F with a shoulder around 430 nm at a 1:8:2.2 molar ratio also indicates such competition. When three equivalents of  $ZnI_2$  are finally reached these shoulders are minimal and the 520-nm peak is maximum. Hence it is very likely that the second and third equivalents of  $ZnI_2$  per BR attach to the second pyrrole ring's site and the site of the two COO-groups on BR as drawn in Figure 23. The one  $Zn^{++}$  on the two COO-groups could be the reason for the 20-nm difference between Szentirmay's 540-nm maximum and the 520-nm maximum found in this study.

In Figure 27 the spectrum of Zn-BRDME is seen shifting to longer wavelengths in curve C and in curve D this complex is seen to maximize. Figure 28 shows the titration of BR with  $Al^{+++}$ . This spectrum of the Al-BR complex shows shifting only when the molar ratio of 1:2:1 for BR:TMG: $Al^{+++}$  was exceeded. The maximum absorbance peak for this Al-BR complex occurred at the molar ratio of 1:2:1.5 at 420 nm. Curve C of Figure 28 represents this maximum. Such a 1:2:1.5 molar ratio for BR to  $Al^{+++}$  indicates that a structure like the one drawn in Figure 24 is feasible for the Al-BR complex. Figure 29 shows that  $Al^{+++}$  can still react with BR even if its preferred COO-

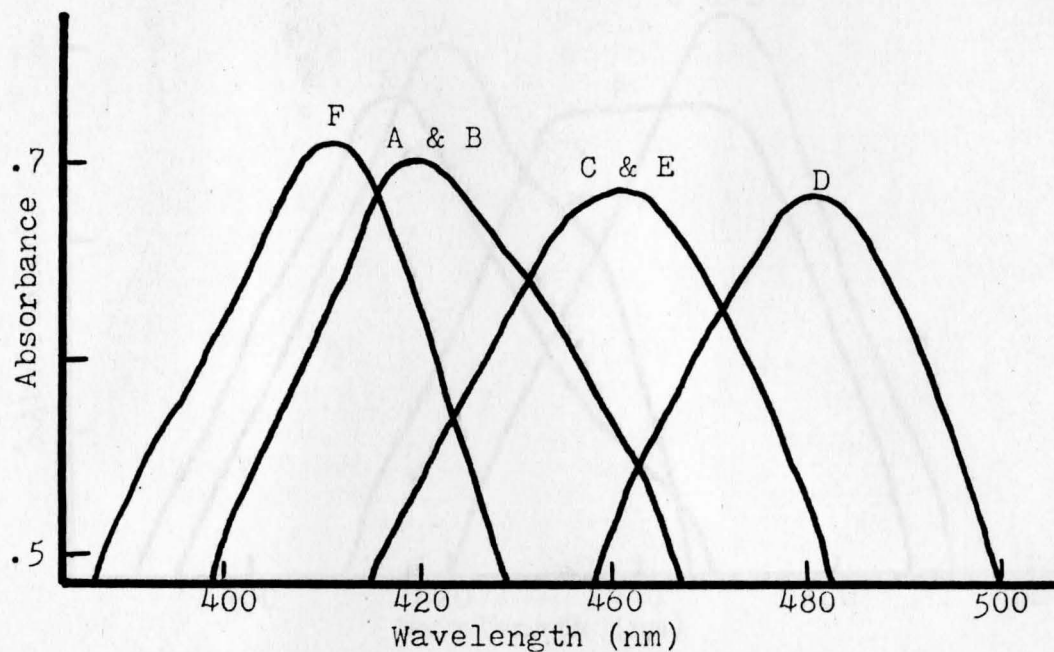


Figure 27. Spectrophotometric Titration of BRDME/TMG with  $ZnI_2/DMF$ .

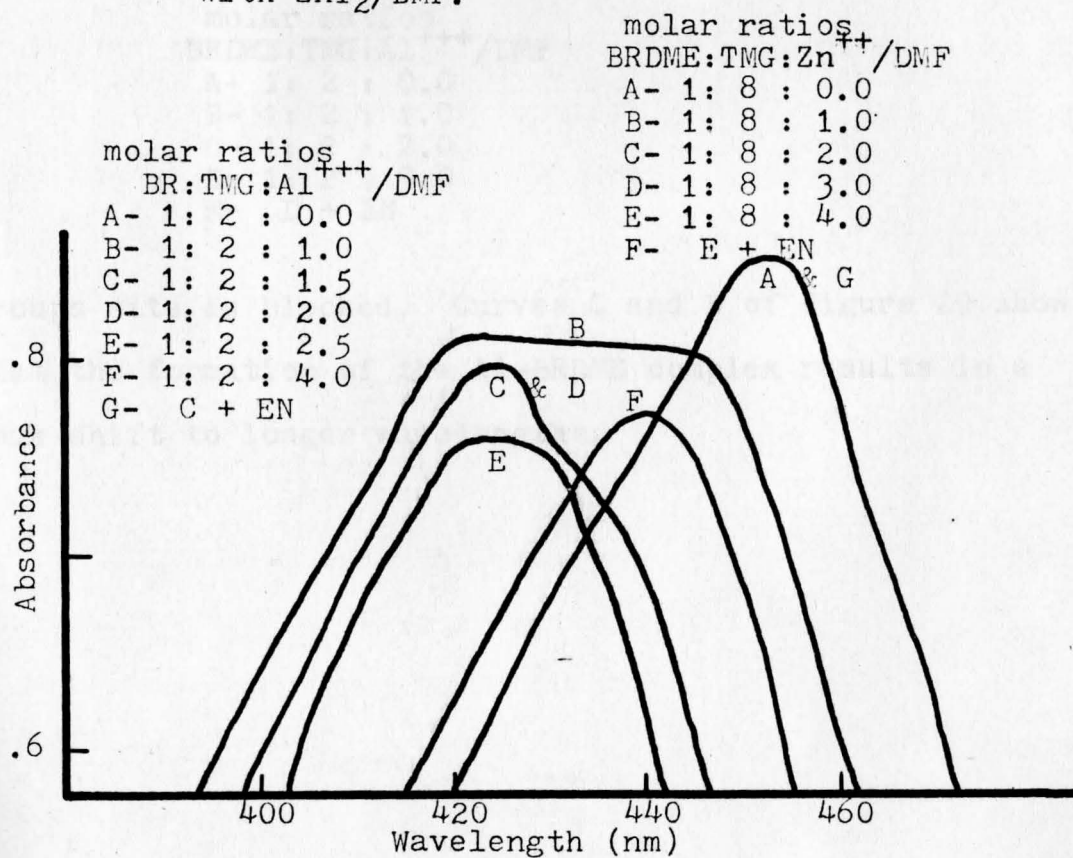


Figure 28. Spectrophotometric Titration of BR/TMG with  $AlCl_3/DMF$ .

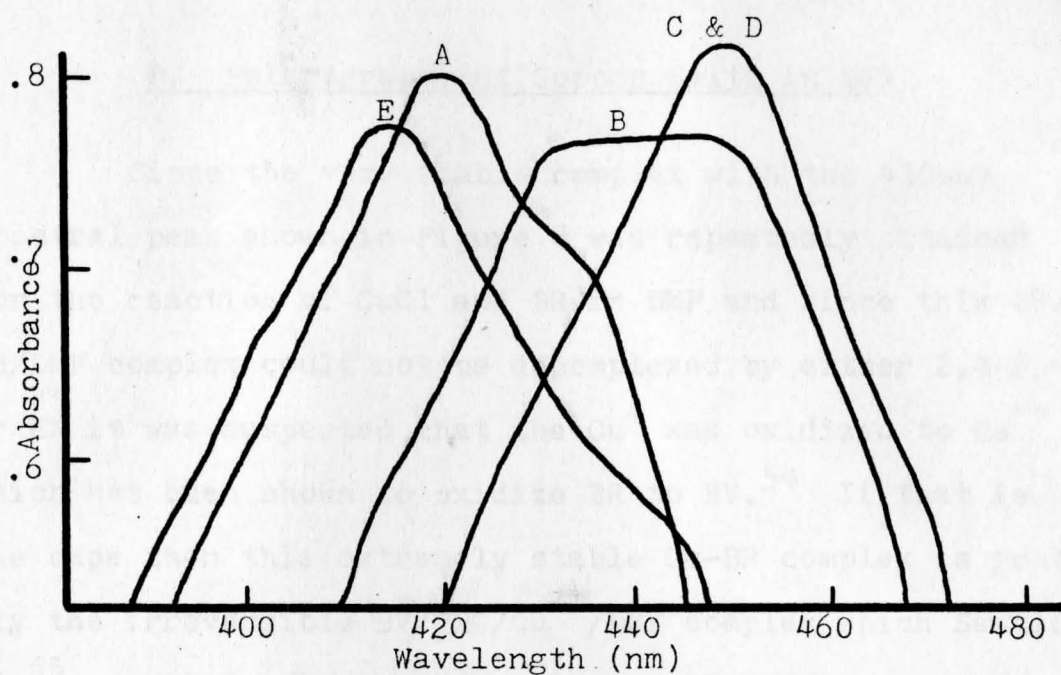


Figure 29. Spectrophotometric Titration of BRDME/TMG with  $\text{AlCl}_3/\text{DMF}$ .

molar ratios  
 BRDME:TMG: $\text{Al}^{+++}/\text{DMF}$   
 A- 1: 2 : 0.0  
 B- 1: 2 : 1.0  
 C- 1: 2 : 2.0  
 D- 1: 2 : 3.0  
 E- D + EN

groups site is blocked. Curves C and D of Figure 29 show that the formation of the  $\text{Al}$ -BRDME complex results in a peak shift to longer wavelengths.

### F. Polarography of Copper Salts in DMF

Since the very stable complex with the 430-nm spectral peak shown in Figure 8 was repeatedly obtained for the reaction of CuCl and BR in DMF and since this BR/TB/DMF complex could not be decomplexed by either 2,4-PDO or EN it was suspected that the  $\text{Cu}^+$  was oxidized to  $\text{Cu}^{++}$  which has been shown to oxidize BR to BV.<sup>54</sup> If that is the case then this extremely stable Cu-BR complex is probably the irreversible BV/TMG/ $\text{Cu}^{++}$ /DMF complex which Sentir-may<sup>55</sup> reported. Polarograms, Figures 30 and 31, were run on CuCl and  $\text{CuCl}_2$  in DMF to test the oxidation states of these two salts in DMF. The results of these two polarograms were that the copper waves for both  $\text{Cu}^+$  and  $\text{Cu}^{++}$  were almost identical. This strongly indicates that in fact  $\text{Cu}^+$  is quickly oxidized to  $\text{Cu}^{++}$  in DMF as was suspected. Also  $\text{Mg}(\text{ClO}_4)_2$ , labeled an oxidizing agent, exhibited irreversible spectral behavior similar to copper upon complexation with BR. Perchlorates in general tended to oxidize BR.

For some metal ions BR complexes were able to be formed when the metal salts were added to a BR/TMG/DMF solution in a solid form; but when these same salts were put into a DMF solution before they were added to the BR/TMG/DMF solution, often irreversible spectral curves similar to the 430-nm Cu-BR curve resulted. When it was attempted to quantitatively titrate  $\text{CdAc}_2 \cdot 2\text{H}_2\text{O}$  and  $\text{SnCl}_2 \cdot 2\text{H}_2\text{O}$  this



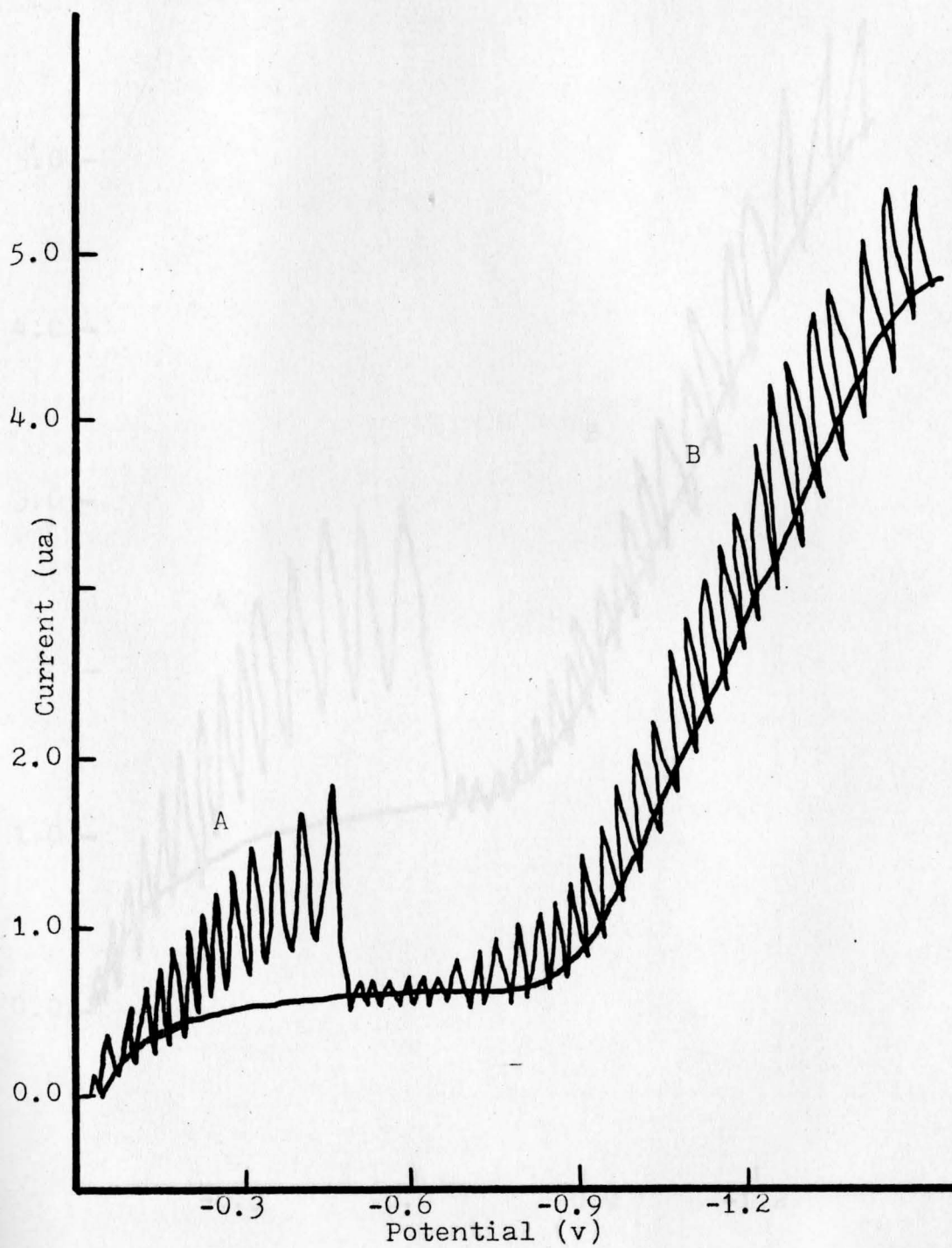


Figure 30. Polarogram of  $\text{CuCl}$  in  $\text{DMF}$ .  
A-  $\text{Cu}$  wave B-  $\text{O}_2$  wave

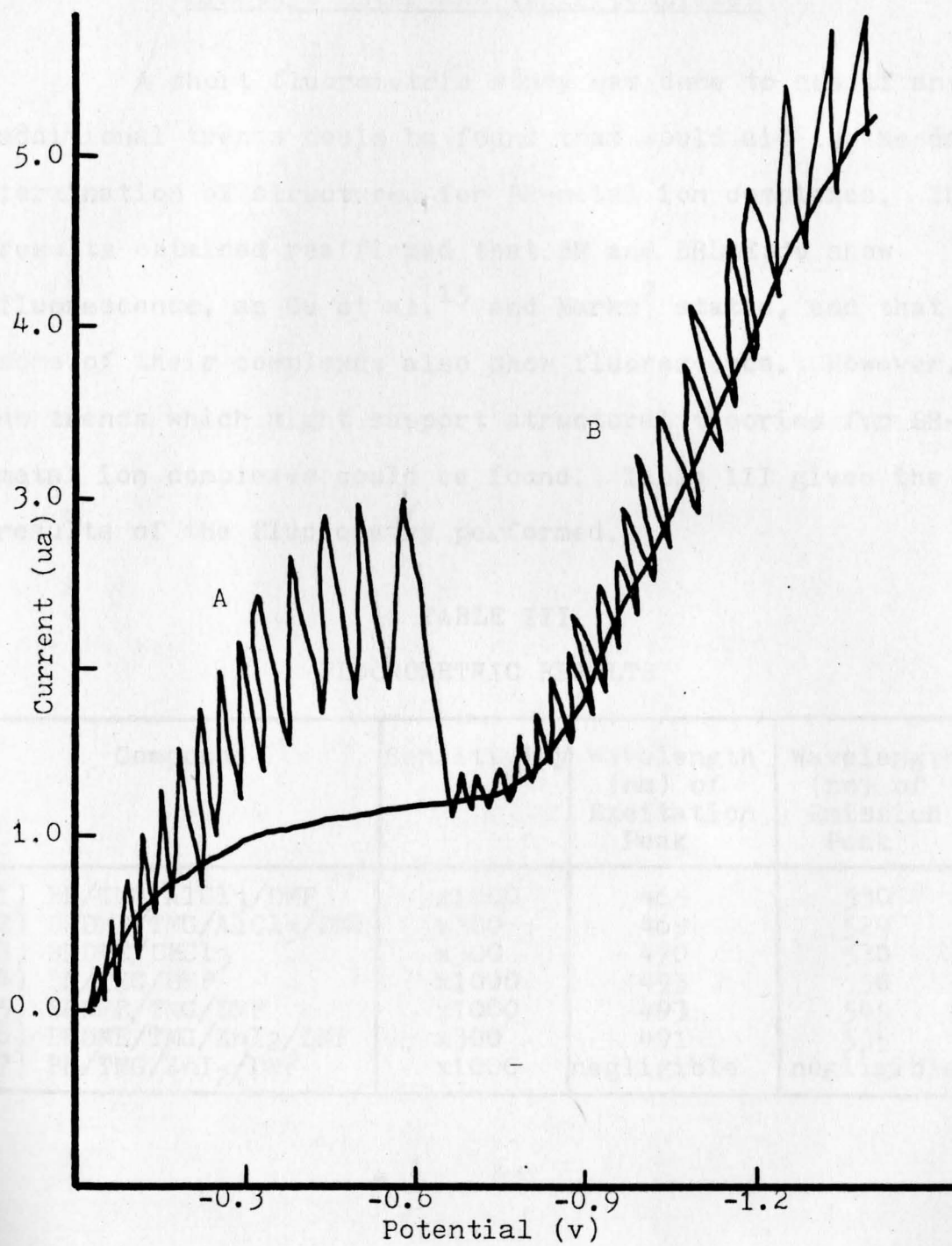


Figure 31. Polarogram of  $\text{CuCl}_2$  in DMF.  
A-  $\text{Cu}^{++}$  wave    B-  $\text{O}_2$  wave

phenomenon occurred.

G. Fluorometry of Bilirubin and Bilirubin Dimethyl Ester and Their Complexes

A short fluorometric study was done to see if any additional trends could be found that would aid in the determination of structures for BR-metal ion complexes. The results obtained reaffirmed that BR and BRDME do show fluorescence, as Cu et al.<sup>15</sup> and Marks<sup>7</sup> stated, and that some of their complexes also show fluorescence. However, no trends which might support structural theories for BR-metal ion complexes could be found. Table III gives the results of the fluorometry performed.

TABLE III  
FLUOROMETRIC RESULTS

Compound	Sensitivity	Wavelength (nm) of Excitation Peak	Wavelength (nm) of Emission Peak
1) BR/TMG/AlCl <sub>3</sub> /DMF	x1000	465	530
2) BRDME/TMG/AlCl <sub>3</sub> /DMF	x300	469	529
3) BRDME/CHCl <sub>3</sub>	x300	470	530
4) BR/TMG/DMF	x1000	493	550
5) BRDME/TMG/DMF	x1000	493	545
6) BRDME/TMG/ZnI <sub>2</sub> /DMF	x300	491	535
7) BR/TMG/ZnI <sub>2</sub> /DMF	x1000	negligible	negligible

## CHAPTER V

## DISCUSSION AND CONCLUSIONS

BR and BRDME complexes with metal ions have been prepared and studied in DMF. Theoretical structures, deduced primarily from experimental data, are proposed. Figures 22, 23 and 24 show these structures. BR-Mg<sup>++</sup>, Al<sup>+++</sup>, Ag<sup>+</sup>, Sn<sup>++</sup>, Pb<sup>++</sup>, Zn<sup>++</sup> and Cd<sup>++</sup> complexes were reproducibly made and decomplexed in DMF. The first five metals, Mg<sup>++</sup> through Pb<sup>++</sup>, shifted the absorbance peak of BR from 450 nm to 420 nm while Zn<sup>++</sup> and Cd<sup>++</sup> shifted the BR absorbance peak to 520 nm. Absorbances at longer wavelengths correspond to lower energies and greater molecular stabilities. Similarly more electron dispersion corresponds to less energy and absorbance peaks at longer wavelengths<sup>56</sup> as was seen in the Zn-BR complex. Spectrophotometric titrations greatly aided in discerning BR-metal ion structures by providing molar ratios of BR:metal ions.

Three important considerations were looked at before BR-metal complexation was attempted. The first includes the realization that protons must be removed from BR before metal ions will complex it. Also metal ions, Lewis acids, often required neutralization before a reaction with BR occurred. Therefore acid-base equilibria was considered. Quantitatively two BR protons were re-

moved with TMG and four BR protons with TB. When attempting to form BR-metal complexes, specific quantities of base were critical. Also, in order to maximize absorbance peaks for particular complexes, specific amounts of base were required.

The second important consideration in understanding BR-metal reactions was the type of metal salt used and the state of the salt when added to a BR/TMG/DMF solution. Some metal salts formed BR-metal complexes when added to a BR/TMG/DMF solution as solids. But when the same salt was added to BR after the salt was already dissolved in DMF, little or no complexing occurred. Also two different salts containing the same metal ion often gave different results. Possibly different ligands or anions on a given metal ion affected BR's combining with that metal ion differently. It is highly probable that the oxidation states of some metal ions were changed when put into DMF before the BR-metal reaction could take place. Such an oxidation theory resulted from a short polarographic study done on copper in DMF.

The third consideration concerned the purity of the solvent, DMF. Many metal ions complex amines. Water, light and heat were found to accelerate the decomposition of DMF into amines which compete with BR for metal ions. Therefore painstaking care needed to be taken in the purification and storage of DMF.

Two additional studies were performed that support

the theory that different structures exist for Al-type and Zn-type BR complexes. The first involved the preparation and complexation of BRDME. It is known that methylation of BR occurs on the two COO-groups of BR.<sup>16</sup> BRDME/TMG/DMF absorbs light at 420 nm like BR/TMG/Al<sup>+++</sup>/DMF. Disturbance of BR's intramolecular hydrogen bonding was presented as an explanation for both BRDME and Al-BR absorbing light at shorter wavelengths than BR. Using the two methyl groups as blocking groups on the two COO-groups of BR, Zn- and Al-BRDME complexes were made. The Zn-BRDME complex shifted the BRDME 420-nm peak to a longer wavelength as did the formation of the Zn-BR complex; however the Al-BRDME complex shifted the BRDME 420-nm peak to a longer wavelength unlike what occurred in the formation of the Al-BR complex. This denotes that a Zn<sup>++</sup> preferentially attaches to the pyrrole nitrogens of BR while an Al<sup>+++</sup> can attach these nitrogens but prefers the COO-groups of BR.

The second additional study involved the decomplexation of the stable BR-complexes formed. EN with two nitrogens per molecule easily broke up any Zn-type complexes but sometimes failed to decomplex Al-type ones; and 2,4-PDO with two oxygens per molecule easily decomplexed all Al-type complexes and most Zn-types. Nevertheless, the fact that BR-metal complexes could be decomplexed strongly indicates that a BR-metal reaction was the cause of the spectral shifts observed. Finally a spectrofluorometric study of BR, BRDME and their complexes was under-

taken with inconclusive results.

The methods used in this study, although indirect, seem to be quite meaningful in the further elucidation of the structures of BR-metal ion complexes. Certainly this study is only a small step in the overall picture of BR-metal ion complexation chemistry. Many more BR-metal ion complexes are yet to be found. Perhaps some of these BR-metal complexes presented here or yet to be found can be crystallized and subjected to more direct analysis such as X-ray crystallography or infrared analysis. Also, the complexes and theories about them put forth here could possibly be used to develop better analytical methods of determining BR levels in the body and perhaps even be used in the development of better methods of controlling BR levels in jaundice patients. Jirsa et al.<sup>8</sup> concluded that BRDME could not be excreted from the body because the normal sites of conjugation of glucuronic acid with BR are occupied. Because of the importance of bile pigments in living systems, because of the similarity of the structure of BR as a polydentate ligand to the porphyrins, and because the active sites of many enzymes are thought to involve metal ion complexation, further study of BR as a polydentate ligand by any method could become quite valuable in the overall understanding of the physiology of living systems.

## REFERENCES

1. R. Szentirmay, Masters Thesis, Youngstown State University, Youngstown, Ohio, 1973, pp. 6-13.
2. J. D. Van Norman and R. Szentirmay, Anal. Chem., 46, 1456 (1974).
3. J. D. Van Norman and R. Szentirmay, Bioinorg. Chem., 4, 37 (1974).
4. J. D. Van Norman, Anal. Chem., 45, 173 (1973).
5. Reference 1, pp. 77-87.
6. Reference 1, p. 4.
7. G. Marks, Senior Research Paper, Youngstown State University, Youngstown, Ohio, 1976.
8. M. Jirsa, J. P. Dickinson and G. H. Lathe, Nature, 220, 1322 (1968).
9. I. M. Kolthoff, E. B. Sandell, E. J. Meehan and S. Bruckenstein, Quantitative Chemical Analysis. Forth Edition. The Macmillan Company, New York, New York, 1969, pp. 102-109.
10. I. M. Kolthoff, M. K. Chantooni and H. Smagowski, Anal. Chem., 42, 1622 (1970).
11. J. J. Lee, L. H. Daly and M. L. Cowger, Res. Commun. Chem. Path. Pharm., 2, 763 (1974).
12. R. A. Velapoldi and O. Menis, Clin. Chem., 17, 1165 (1971).
13. D. W. Hutchinson, B. Johnson and A. J. Knell, Biochem. J., 133, 399 (1973).
14. C. C. Kuenzle, R. R. Pelloni and M. H. Weibel, Biochem. J., 133, 1147 (1972).
15. A. Cu, G. Bellah and D. A. Lightner, J. Amer. Chem. Soc., 97, 2579 (1975).
16. D. W. Hutchinson, B. Johnson and A. J. Knell, Biochem. J., 133, 493 (1973).
17. F. Cotton and G. Wilkinson, Advanced Inorganic Chemistry. Second Edition. Interscience Publishers, New York, 1966, pp. 434-445.



## REFERENCES (CONT'D)

18. P. J. Durrant and B. Durrant, Introduction to Advanced Inorganic Chemistry. Second Edition. John Wiley & Sons, Inc., New York, 1956, pp. 564-579.
19. J. C. Bailar, Jr., The Chemistry of the Coordination Compounds. Second Printing. Reinhold Publishing Corporation, New York, 1956, pp. 164-579.
20. M. Mercer and M. Truter, J. C. S. Dalton, 20, 2215 (1973).
21. L. Pauling, The Nature of the Chemical Bond. Third Edition. Cornell University Press, Ithaca, New York, 1960, pp. 108-182.
22. P. Monitto and D. Monti, J. C. S. Chem. Comm., 4, 122 (1976).
23. C. C. Kuenzle, M. H. Weibel and R. R. Pelloni, Biochem. J., 133, 364 (1973).
24. Reference 19, pp. 174-175.
25. Reference 19, p. 164.
26. Reference 19, p. 164.
27. Reference 19, p. 168.
28. Reference 21, pp. 111-116 and 158.
29. Reference 17, p. 439.
30. Reference 18, p. 565.
31. Reference 21, p. 158.
32. Reference 18, p. 571.
33. Reference 18, p. 578.
34. Reference 21, p. 150.
35. Reference 9, pp. 105-108.
36. Reference 9, p. 108.

## REFERENCES (CONT'D)

37. Reference 9, p. 1150.
38. Reference 9, pp. 959-960.
39. Reference 9, p. 888.
40. Reference 1, p. 23.
41. Reference 1, p. 50.
42. Reference 1, p. 86.
43. Reference 1, p. 113.
44. Reference 1, pp. 77-91.
45. Reference 7, pp. 20-22.
46. Reference 1, pp. 77-91.
47. Reference 19, pp. 672-673, 690-691 and 741.
48. Reference 9, pp. 105-107.
49. Reference 18, pp. 571 and 578-579.
50. Reference 19, p. 253.
51. Reference 19, p. 175.
52. Reference 19, p. 175.
53. Reference 1, p. 80.
54. Reference 1, p. 115.
55. Reference 1, p. 117.
56. Reference 9, pp. 959-960.